(12) INTERNATIONAL APPLICATION PUBLISHED UNDER THE PATENT COOPERATION TREATY (PCT)

(19) World Intellectual Property Organization
International Bureau

(43) International Publication Date
5 December 2002 (05.12.2002)

PCT

(10) International Publication Number
WO 02/097444 A2

(51) International Patent Classification[7]: G01N 33/68

(21) International Application Number: PCT/US02/17212

(22) International Filing Date: 30 May 2002 (30.05.2002)

(25) Filing Language: English

(26) Publication Language: English

(30) Priority Data:
60/295,456 31 May 2001 (31.05.2001) US

(71) Applicant *(for all designated States except US)*: **ARETE ASSOCIATES** [US/US]; 5000 Van Nuys Boulevard, Suite 420, Sherman Oaks, CA 91403 (US).

(72) Inventors; and

(75) Inventors/Applicants *(for US only)*: **ORSER, Cindy** [US/US]; 915 Ridge Drive, McLean, VA 22101 (US). **GROSSET, Anne** [US/US]; 205, route de Bardonnex, CH-1257 La Croix-de-Rozon (CH). **DAVIDSON, Eugene** [US/US]; 5506 Nebraska Avenue, NW, Washington, DC 20015 (US).

(74) Agent: **LIPPMAN, Peter, I.**; Ashen & Lippman, 4385 Ocean View Boulevard, Montrose, CA 91020 (US).

(81) Designated States *(national)*: AE, AG, AL, AM, AT, AU, AZ, BA, BB, BG, BR, BY, BZ, CA, CH, CN, CO, CR, CU, CZ, DE, DK, DM, DZ, EC, EE, ES, FI, GB, GD, GE, GH, GM, HR, HU, ID, IL, IN, IS, JP, KE, KG, KP, KR, KZ, LC, LK, LR, LS, LT, LU, LV, MA, MD, MG, MK, MN, MW, MX, MZ, NO, NZ, OM, PH, PL, PT, RO, RU, SD, SE, SG, SI, SK, SL, TJ, TM, TN, TR, TT, TZ, UA, UG, US, UZ, VN, YU, ZA, ZM, ZW.

(84) Designated States *(regional)*: ARIPO patent (GH, GM, KE, LS, MW, MZ, SD, SL, SZ, TZ, UG, ZM, ZW), Eurasian patent (AM, AZ, BY, KG, KZ, MD, RU, TJ, TM), European patent (AT, BE, CH, CY, DE, DK, ES, FI, FR, GB, GR, IE, IT, LU, MC, NL, PT, SE, TR), OAPI patent (BF, BJ, CF, CG, CI, CM, GA, GN, GQ, GW, ML, MR, NE, SN, TD, TG).

**Published:**
— *without international search report and to be republished upon receipt of that report*

*[Continued on next page]*

(54) Title: MISFOLDED PROTEIN SENSOR METHOD

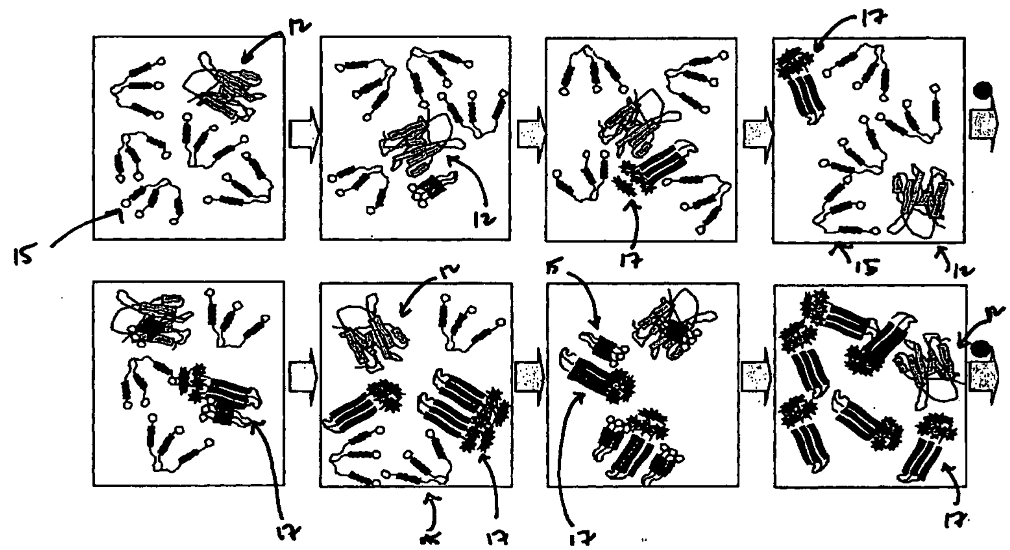

(57) Abstract: A catalytic conformational sensor method for detecting abnormal proteins and proteinaceous particles. The method is based on the interaction of a peptide fragment or probe with an abnormal proteinaceous particle. The interaction catalyzes transformation of the probe to a predominately beta sheet conformation and allows the probe to bind to the abnormal proteinaceous particle. This in turn, catalyzes propagation of a signal associated with the test sample-bound probe. As a result signals can be propagated even from samples containing very low concentrations of abnormal proteinaceous particles. The peptide probes can be designed to bind to a desired peptide sequence or can even be based on dendrimer structure to control further aggregate propagation.

WO 02/097444 A2

*For two-letter codes and other abbreviations, refer to the "Guidance Notes on Codes and Abbreviations" appearing at the beginning of each regular issue of the PCT Gazette.*

# MISFOLDED PROTEIN SENSOR METHOD

## BACKGROUND

### 1. FIELD OF THE INVENTION

This invention relates generally to a catalytic conformational sensor method and application of such method for detecting proteins and proteinaceous particles; and more particularly to detecting misfolded or disease-associated proteins and proteinaceous particles.

### 2. RELATED ART

This document claims priority of United States provisional patent application serial number 60/295,456 filed on May 31, 2001, with respect to subject matter therein; said provisional application fully being incorporated herein.

The present invention detects misfolded or abnormal conformations of proteins or peptides such as those contributing to "folding diseases". The "folding diseases" are characterized by proteins with destabilizing conformers which tend to aggregate and eventually form toxic plaques in brain and other tissue. See Bucciantini, M., *et al.* (2002) *Inherent Toxicity of Aggregates Implies a Common Mechanism for Protein Misfolding Diseases*. Nature 416:507-511.

These "folding diseases" can be hard to diagnose since the disease symptoms may be latent where the aggre-

gates are slowly building up over time and go through stages of increased aggregation leading to fibril formation and eventual plaque deposition leading to impairment of cellular viability. Such misfolding of peptides and aggregate formation is believed to play a key role in Alzheimer's disease where beta-amyloid protein (or A beta, a 39-42 residue peptide) forms fibrillar deposits upon a conformer change; Huntington's disease where insoluble protein aggregates are formed by expansion of poly-glutamine tracts in the N-terminus of huntingtin (Htt), an antiapoptotic neuronal protein; and noninfectious cancers such as in cases where tumor-associated cell surface NADH oxidase (tNOX) has prion-like properties such as proteinase$^R$, ability to form amyloid filaments and the ability to convert the normal NOX protein into tNOX. See Kelker, *et al. Biochemistry* (2001) 40:7351-7354. for more information on tNOX.

The present invention, however, is not limited to the detection of proteins or peptides in folding-disease or infectious samples. It also includes detection of proteinaceous particles such as prions. Prions are small proteinaceous particles with no nucleic acids, thus are resistant to most nucleic-acid modifying procedures and proteases. The normal prion (PrP) protein is a cell-surface metalloglyroprotein that is mostly an alpha-helix and loop structure as shown in Fig. 8, and is usually expressed in the central nevrvous and lymph systems. It's proposed function is that of an antioxidant and cellular homeostasis.

The abnormal form of the PrP, however, is a conformer which is resistant to proteases and is predominantly beta-sheet in its secondary structure as shown in Fig. 9. It is believed that this conformational change in secondary

structure is what leads to the aggregate and eventual neurotoxic plaque deposition in the prion-disease process.

The abnormal prion are infectious particles that play key roles in the transmission of several diseases such as Creutzfeldt-Jakob syndrome, chronic wasting disease (CWD), nvCJD, transmissible spongiform encephalopathy (TSE), Mad Cow disease (BSE) and scrapie a neurological disorder in sheep and goats[1].

Diseases caused by prions can be hard to diagnose since the disease may be latent where the infection is dormant, or may even be subclinical where abnormal prion is demonstrable but the disease remains an acute or chronic symptomless infection. Moreover, normal homologues of a prion-associated protein exist in the brains of uninfected organisms, further complicating detection.[2] Prions associate with a protein referred to as PrP 27-30, a 28 kdalton hydrophobic glycoprotein, that polymerizes (aggregates) into rod-like filaments, plaques of which are found in infected brains. The normal protein homologue differs from prions in that it is readily degradable as opposed to prions which are highly resistant to proteases. Some theorists believe that prions may contain extremely small amounts of highly infectious nucleic acid, undetectable by conventional assay methods.[3] As a result, many current techniques used to detect the presence of prion-related infections rely on the gross morphology changes in the brain and immunochemistry techniques that are generally applied only after symptoms have already manifest them-

---

[1] Clayton Thomas, *Tabor's Cyclopedic Medical Dictionary* (Phil., F.A. Davis Company, 1989), at 1485.

[2] Ivan Roitt, et al., *Immunology* (Mosby-Year Book Europe Limited, 1993), at 15.1.

[3] Benjamin Lewin, *Genes IV* (Oxford Univ. Press, New York, 1990), at 108.

selves. Many of the current detection methods rely on antibody-based assays or affinity chromatography using brain tissue from dead animals and in some cases capillary immunoelectrophoresis using blood samples.

The following is an evaluation of current detection methods.

- o *Brain Tissue Sampling*. Cross-sections of brain can be used to examine and monitor gross morphology changes indicative of disease states such as the appearance of spongiform in the brain, in addition to immunohistochemistry techniques such as antibody-based assays or affinity chromatography which can detect disease-specific prion deposits. These techniques are used for a conclusive bovine spongiform encephalopathy (BSE) diagnosis after slaughter of animals displaying clinical symptoms. Drawbacks of tissue sampling include belated detection that is possible only after symptoms appear, necessary slaughter of affected animals, and results that takes days to weeks to complete.

- o *Prionic-Check* also requires liquified-brain tissue for use with a novel antibody under the Western Blot technique. This test is as reliable as the immunochemistry technique and is more rapid, yielding results in six to seven hours, but shares the drawbacks of the six-month lag time between $PrP^{S}$ accumulation (responsible for the gross morphology changes) in the brain and the display of clinical symptoms, along with the need for slaughter of the animal to obtain a sample.

- *Tonsillar Biopsy Sampling.* Though quite accurate, it requires surgical intervention and the requisite days to weeks to obtain results.

- *Body Fluids: Blood and Cerebrospinal Sampling.* As in the above detection methods, results are not immediate

- *Electrospray ionization mass spectrometry (ESI-MS), nuclear magnetic resonance NMR, circular dichroism (CD) and other non-amplified structural techniques.* All of these techniques require a large amount of infectious sample, and have the disadvantage of requiring off-site testing or a large financial investment in equipment.

The following is a survey of currently approved and certified European Union (EU) prion-detection tests.

- Prionics -in Switzerland. The test involves Western blot of monoclonal antibodies (MABs) to detect PrP in brain tissue from dead animals in seven to eight hours.

- Enfer Scientific -in Ireland. The test involves ELISA-based testing on spinal cord tissue from dead animals in under four hours.

- CEA -in France. The test involves a sandwich immunoassay using two monoclonals on brain tissue collected after death in under twenty-four hours.

The EU Commission's evaluation protocol has sensitivity, specificity and detection limits and titre. The

sensitivity of a test is the proportion of infected reference animals that test positive in the assay. It previously used 300 samples from individual animals to assess this element. The specificity of a test is the proportion of uninfected reference animals that test negative in the assay. Previously used 1,000 samples from individual animals for this purpose. In order to test detection limits, various dilutions ranging from $10^0$ to $10^{-5}$ of positive brain homogenate were used. A table showing an evaluation of EU test results is shown in Fig. 12. Even with high degrees of sensitivity and specificity, however, the fact remains that these tests must be performed post-mortem and require working with large amounts of highly infectious biohazard materials.

The Center for Disease Control (CDC) classifies prions as Risk Group 2 agents requiring Biosafety Level 2 (BSL2) containment. As a result many of the above operations are carried out under BSL2 physical containment with elevated safety practices more typical of a BSL3 lab. Prions can be inactivated by fresh household bleach, 1 molar NaOH, 4 molar guanidine reagents, or phenol followed by 4.5 hours of autoclaving at 132°C. Procedures involving brain tissue from human patients with neurological degenerative disorders pose special challenges and should be handled with the same precautions as HIV+ human tissue. Thus, working with large amounts of such biohazardous materials can be an obstacle to quick and simple testing of mass quantities or assembly-line samples as well as cumbersome even for small applications.

In addition to working with relatively large amounts of biohazardous materials and taking several hours to weeks

for detection, many of the prior art methods have the added difficulty that they are performed post mortem.

As can now be seen, the related art remains subject to significant problems, and the efforts outlined above — although praiseworthy — have left room for considerable refinement. The present invention introduces such refinement.

## SUMMARY OF THE DISCLOSURE

The present invention is based on the interaction between low concentration levels of abnormal proteinaceous particles and a peptide fragment or probe to induce transformation and propagation of the probe bound to the abnormal proteinaceous particles initially present within a test sample. Thus, in a preferred embodiment, infectious levels of a test sample can be propagated even from low concentrations.

The present invention uses catalytic propagation to exploit conformational changes in proteins associated with a particular disease process, such as transmissible spongiform encephalopathy (TSE). Catalytic propagation basically amplifies the number of existing protein fragments causing aggregates to form. The aggregates of conformationally changed protein fragments are then easily detected using common analytical techniques.

As a result, the present invention allows testing to be done using rapid and cost-effective analytical tech-

niques, even on, heretofore difficult to detect, small sample sizes and is widely applicable to tissues and body fluids other than those found in brain. Results of the present invention can easily and immediately interpreted using familiar analytical instrumentation. Additionally, the present invention can amplify a weak signal, thus can be successfully applied to small or weak samples such as those associated with body fluids; thereby opening the door to analysis of tissues and fluids for the elusive diseases discussed above. Moreover, this allows the method to be relatively noninvasive in that it does not need to be performed post-mortem; and because it does not need to be performed post-mortem it can be applied to presymptomatically.

The foregoing may be a description or definition of the first facet or aspect of the present invention in its broadest or most general terms. Even in such general or broad form, however, as can now be seen the first aspect of the invention resolves the previously outlined problems of the prior art.

Because the present invention allows detection using samples with very low levels of infectious agents and involves amplifying a peptide probe as opposed to a whole potentially infectious protein, many of the previous biohazard-handling concerns are reduced.

Now turning to another of the independent facets or aspects of the invention: in preferred embodiments of this facet, the peptide probes are designed for the detection of a desired sequence and so have adaptable levels of selectivity and specificity built into the method. Also, in-

trinsic optical fluors such as pyrene can be designed into the peptide probe allowing simple, single step optical detection of the abnormal proteinaceous particles.

All of the foregoing operational principles and advantages of the present invention will be more fully appreciated upon consideration of the following detailed description, with reference to the appended drawings, of which:

## BRIEF DESCRIPTION OF THE DRAWINGS

Fig. 1 is a pictoral representation of conformers of transmissible spongiform encephalopathies (TSE) and probes in the form of labeled peptides and labeled dendrimers;

Fig. 2 is a pictoral representation of TSE protein detection schema;

Fig. 3 is a graph showing the conformational changes associated with a poly-L-lysine test peptide using circular dichroism;

Fig. 4 is a graph comparing the circular dichroism results of the poly-L-lysine test peptide at different temperatures and pH;

Fig. 5 is a table comparing the circular dichroism results of the poly-L-lysine test peptide at different temperatures and pH;

Fig. 6 is a graph of data for fluorescence resonance energy transfer (FRET) experiments for proximal and distal locations in an α-helical bundle structure undergoing conformational change;

Fig. 7 is a graph of the driving force necessary to overcome the energy difference between two different

Fig. 8 is a structural diagram of a normal PcP protein, a cell-surface metallo-glycoprotein that is expressed in the central nervous and lymphatic systems, and that is characterized as having mostly an alpha-helix and loop structure;

Fig. 9 is a structural diagram of the PcP protein that has shifted to a predominately beta structure in which it is likely for form aggregates and neurotoxic fibrils eventually leading to plaque deposition;

Fig. 10 is a pictoral representation of amplification of signal and propagation of conformational change without increased aggregation by the addition of dendrimers of the invention to a test sample;

Fig. 11 is a structural diagram of proteins used in the current prior art prion-diagnostic market; wherein Fig.11a on the left shows the PrPsens protein molecule and Fig. 11b on the right shows a PrPres protein molecule;

Fig. 12 is a table evaluating the current prior art in European Union certified prion-diagnostic tests

Fig. 13 is a comparison showing selected PrP sequences among six different species;

Fig. 14 shows peptide sequences for the synthetic peptide probes Seq. 19 and Seq. 14 of this invention;

Fig. 15 is a graph of fluorescence detection experimental results showing the effects of peptide concentration;

Fig. 16 is a graph of fluorescence detection experimental results showing the effects of peptide concentration likely showing excimer emission at approximately 460 nanometers (nm);

Fig. 17 is a graph of fluorescence detection experimental results showing pyrene's excitation of fluorescence;

Fig. 18 is a graph of fluorescence detection experimental results showing pyrene's excitation spectra for fluorescence at 398 and approximately 460 nm;

Fig. 19 is a graph comparing the circular dichroism results of several peptides ranging in concentration from 20 to 100 milli Molar (mM) under varying buffer conditions;

Fig. 20 is a graph comparing the circular dichroism results of several peptides including the synthetic peptides of Seq. 19 and Seq. 14 under varying buffer conditions;

Fig. 21 shows experimental results of the conformational lability of the synthetic peptides. Fig. 21a on the left shows that Seq. 14 assumes a beta-sheet conformer while the longer analog, Seq. 19 remains coiled. Fig. 21b on the right shows that addition of Seq. 14 to Seq. 19 initiates a phase shift to beta-sheet form;

Fig. 22 is a conceptual illustration of a comparison of where Seq. 19 and Seq. 14 overlap in structure;

Fig. 23 is a graph of experimental results showing that peptides can self-associate;

Fig. 24 is a graph of fluorescence data showing the efficiency of excimer formation under low concentrations;

Fig. 25 is a graph of fluorescence experimental results showing the effect of nuclei on self-association due to catalytic conformational transition;

Fig. 26 contains two graphs of fluorescence experimental results showing the interaction of Seq. 19 and Seq. 14 at different ratios; wherein Fig. 26a on the left shows a 1:1 mixture and Fig. 26b on the right shows a 100:1 mixture;

Fig. 27 contains four graphs of fluorescence experimental results showing the effect of nuclei on self-association. Figs. 27a, b, c and d show the results at 24 hours, 48 hours, 144 hours and 336 hours, respectively;

Fig. 28 is a graph of fluorescence experimental results showing the effect of nuclei on self-association due to catalytic conformational transition at 1 hour in Fig. 28a on the left and at 150 hours in Fig. 28b on the right;

Fig. 29 shows peptide sequences for a generalized dendrimer structure of this invention;

Fig. 30 shows a peptide sequence for a preferred embodiment of a specific dendrimer structure of this invention;

Fig. 31 is a conceptual diagram of an experimental device; and

Fig. 32 is a system diagram of preferred embodiments of the invention.

## DETAILED DESCRIPTION OF THE PREFERRED EMBODIMENTS

It is to be understood that the invention is not limited to the examples described herein. All technical and scientific terms used herein have meanings as commonly understood by one of ordinary skill in the art unless otherwise defined. All publications referred to herein are wholly incorporated by reference to describe methods and materials for implementing aspects of the invention.

The present invention detects the presence of abnormal proteins and proteinaceous particles based on a method that utilizes catalytic propagation. Upon interaction of a sample, containing abnormal proteins or proteinaceous particles, with a peptide probe of the invention, the peptide probe undergoes conformational changes resulting in the formation of aggregates. The addition of the abnormal proteins and proteinaceous particles catalyzes the formation of the aggregates and causes further propagation of this conformational transition. The resulting aggregates are then easily detected using common analytical instrumentation and techniques.

The abnormal proteins and proteinaceous particles on which the invention focuses are proteins, protein based chemical structures such as prions and protein subunits such as peptides that are capable of conformational changes that lead to the formation of aggregates and ultimately to disease states.

These proteins and proteinaceous particles form aggregates by shifting from a monomeric to a multimeric state. The shift from one distinct state to the other requires a driving force that is commensurate with the energetic difference between the two conformational states as shown in Fig. 7.

A preferred example of such proteinaceous particles is that of a prion protein. Prions can exist in one of two distinct conformations characterized by having a secondary protein structure that is either predominately alpha-helical or predominately beta-sheet; where the predominately beta-sheet conformation has a much higher preference to exist in a multimeric state. As a result, predominately

beta-sheet (or beta rich) secondary structure is more typical of abnormally folded or disease-causing proteinaceous particles since their preference to aggregate is likely to be disruptive in an *in vivo* environment.

Fig. 1 shows illustrations of both the alpha-helical monomer 10 and the beta-sheet dimer 12 forms of a TSE conformer (or alternative secondary structure). Research has shown that the normal wild-type (wt) form of prion protein ($PrP^{C}$) prefers a monomeric state, while the abnormal, disease-causing form ($PrP^{Sc}$) more readily takes on a multimeric state.[4]

This distinction between the secondary structure of the normal form of prion protein and the abnormal form as well as its propensity to cause aggregation is exploited in the present invention to allow detection of the abnormal form even in samples with very low levels of infectious abnormal protein.

The mechanism of the invention is shown in a schematic in Fig. 2. The top row of the schematic shows an example of an unknown sample of TSE protein represented as containing beta-sheets 12. The beta-sheets are then disaggregated by subjecting the sample to commonly known disaggregation methods such as sonication. This is followed by the addition of labeled peptide probes 14 which are allowed to bind to the sample 12. Presence of the beta-sheet conformation in the sample 12 induces the peptide probes to also shift to beta-sheet formation 16. In this manner the transition to beta-sheet is propagated among the peptide probes 14 thereby causing new aggregates 18 to form. The resulting transition to a predominately beta-sheet form and amplified

---

[4] Fred E. Cohen, et al., *Pathologic Conformations of Prion Proteins* (Annu. Rev. Biochem. 1998) 67: 793-819.

aggregate formation can then easily be detected using common analytical techniques such as light scattering and circular dichroism (CD); and in a particularly preferred embodiment where the peptide probe is fluorescent labeled, fluorescence detection instrumentation can also be used.

The bottom row of Fig. 2 shows an alternative example in which the unknown sample of TSE protein is represented in its normal alpha-helical form 10. For consistency, the sample is subjected to the same disaggregation process described above. Upon addition of the labeled peptide probes 14, neither a transition to beta-sheet form nor binding to the unknown samples occurs. As a result, there is no aggregate fluorescence signal in the case of a labeled peptide probe as well as no detection of aggregate formation by other analytical tools. Based on this schematic, unknown samples can be tested for the presence or absence of such abnormal protein conformations or sequences.

A preferred embodiment of the invention involves the following basic procedures. Peptide probes 14 are selected in order to be added to an unknown or test sample 20 at a later stage in the process. The peptide probes 14 are preferably proteins or peptide sequences that have secondary structures of predominately alpha-helix or random coil. In a particularly preferred embodiment, the peptide probes 14 are peptide fragments consisting of a helix-loop-helix structure as found in lysine. In another particularly preferred embodiment, the peptide probes can be made of a peptide sequence chosen from wild-type (wt) TSE, from a desired species-specific TSE peptide sequence, or even from a selectively mutated TSE sequence that has been mutated in

such a manner as to render it destabilized and noninfectious. Additionally, extrinsic fluors such as pyrene can be added or designed into the peptide probe to allow detection of anticipated conformational changes using common fluorescence detection techniques.

Once a peptide probe 14 is selected, it is added to a test sample 20. Prior to the addition of the peptide probe 14, however, it is preferred to have the sample 20 subjected to disaggregation techniques commonly known in the art, such as sonication. The disaggregation step allows any potentially aggregated sample material 20 to break apart so that these disaggregated sample materials 22 are more free to recombine with the newly introduced peptide probes 14; thereby facilitating the anticipated catalytic propagation.

After the test sample 20 or disaggregated test sample 22 is allowed to interact with the peptide probes 14. The resulting mixture is then subjected to analytical methods commonly known in the art for the detection of aggregates and to fluorescence measurements in cases where fluorescent peptide probes 14 are used.

Unknown or test samples 20 containing any dominant beta-sheet formation characteristic of abnormally folded or disease-causing proteins results in an increase in beta-sheet formation and consequently aggregate formation in the final mixture containing both the test sample 20 and the peptide probes 14. Conversely, unknown or test samples 20 which lack a predominantly beta-sheet secondary structure will neither catalyze a transition to beta-sheet structure 16 nor will propagate the formation of aggregates 18.

One of ordinary skill in the art can appreciate that the means by which the initial conformational change can be triggered in the test samples 20 can be varied as described in the following examples. The binding of a metal ligand could direct a change in the protein scaffolding and favor aggregation. The expression or cleavage of different peptide sequences can promote advanced aggregation leading to fibril and plaque formation. Genetic point mutations can also alter the relative energy levels required of the two distinct conformations, resulting in midpoint shifts in structural transitions. Furthermore, an increase in concentration levels could be sufficient to favor the conformational transition. Regardless of the initial trigger mechanism, however, the disease process in many of the abnormal protein conformations such as in prion-related diseases always involves the catalytic propagation of the abnormal conformation, resulting in transformation of the previously normal protein.

One of ordinary skill in the art can also appreciate that there are many common protein aggregate detection techniques many of which are based on optical measurements. These optical detection techniques include, but are not limited to, light scattering, or hydrophobicity detection using extrinsic fluors such as 1-anilino-8-napthalene sulfonate (ANS) or Congo Red stain, fluorescence proximity probes on the peptide fragments, including fluorescence resonance energy transfer (FRET) & quenching of intrinsic tryptophan fluorescence through either conformational change of monomer or binding at interface in alpha-beta heterodimer; the N-terminal loop region is particlularly

interesting in this regard selective binding to target protein, circular dichroism (CD) monitoring of actual conformation, nuclear magnetic resonance (NMR). Other detection techniques include equilibrium ultracentrifugation or size-exclusion chromotography at the aggregation stage as well as other structural techniques. Examples and explanations of these methods can be found in Freifelder, David. *Physical Biochemistry: Applications to Biochemistry and Molecular Biology*, (W. H. Freeman Press, New York, 2nd ed. 1982). and in Copeland, Robert. *Analytical Methods for Proteins*, (American Chemical Society Short Courses 1994). both of which are wholly incorporated herein as prior art. Many of these enumerated optical and structural methods are rapid, cost-effective and accurate.

Experiments were performed using model systems to show the conformational changes involved in the transition from a predominately alpha-helix to a beta-rich form. The model systems chosen used readily available, nonneurotoxic polyamino acids such as polylysine and polyglutamine. The polyamino acids were chosen because of their availability and more importantly because they are safe to handle thus eliminating the need for special handling or donning cumbersome extra protective gear.

Fig. 3 shows a circular dichroism graph of experimentation with poly-L-lysine 20 micro Molar (µM) 52,000 molecular weight (MW) as a peptide probe. The resulting graphs show:

- Sample 24 which was maintained at pH7, 25°C resulting in a minimum at approximately 205 namometers (nm) indicating random coil structure.

- Sample 26 which was maintained at pH11, 50°C resulting in a minimum at approximately 216 namometers (nm) indicating beta-sheet structure.

- Sample 28 which was a 1:1 combination of samples maintained at pH7, 25°C and at pH11, 50°C resulting in a minimum at approximately 216 namometers (nm) indicating beta-sheet structure.

- Sample 30 which was a 1:1 combination of samples maintained at pH7, 50°C and at pH11, 50°C resulting in a minimum at approximately 216 namometers (nm) indicating beta-sheet structure.

Fig. 4 shows an absorbance graph of experimentation with poly-L-lysine 70 mircomolar (μM) 52,000 molecular weight (MW) as a peptide probe. The resulting graphs show:

- Sample 32 which was maintained at pH 11, 25°C resulting in a plateau at approximately 0.12 indicating predominately alpha-helical structure.

- Sample 34 which was maintained at pH7, 50°C resulting in a a plateau at approximately 0.22 indicating random coil structure.

- Sample 36 which was a 10:1 combination of samples maintained at pH7, 50°C and at pH11, 50°C resulting in a steeper incline from approximately 0.22 to 0.33 indicating an accelerated transition from random coil to beta-sheet structure.

- Sample 38 which was a 10:1 combination of samples maintained at pH7, 25°C and at pH11, 50°C resulting in a gradual incline from approximately 0.22 to 0.26 indicating a transition from random coil to beta-sheet structure.

Fig. 4 shows general circular dichroism results of experimentation with poly-L-lysine at varying temperatures and pH indicating its potential for transitioning from random coil to beta-sheet under the varying environmental conditions. The results indicate that both temperature and pH play an important role in the transition.

The observations based on all of the modeling experimentation described above show that the addition of a relatively small amount of beta-sheet peptide to random coil sample can result in a shift towards a beta-rich conformation and such changes can be accelerated depending on the temperature and pH environment of the samples.

Fig. 6 shows experimentation results using pyrene as a fluorescent probe in proximal and distal locations in an alpha helical bundle structure undergoing conformational change. The pyrene excimer formation 42 is shown at 480 nm and the spectra for a predominately alpha-helical structure 40 is contrasted as well. Those skilled in the art would appreciate that other fluorescent probes such as FITC can also be used.

A primary objective of this invention also encompasses use of the catalytic propagation of conformational change to directly correlate the measures of abnormal prion pres-

ence with levels of infectivity. For this reason we favor implementation of the invention in a manner where there is no increase in resulting infectious products as a result of the propagation. This can be achieved by placing a "break" in the links between the chain of infection, transmission and propagation of the abnormal form. Such a "break" must occur at the transitional stage between the dimer and multimer forms of the aggregate. The physical formation of the multimer form can be blocked by simply impeding the step which leads to its formation. This may be done, preferably by using a large pendant probe or by a neutral "blocker" segment, bearing in mind that probes on linkers or "tethers" are more likely to encounter each other and thus result in amplifying the signal.

In a particularly preferred embodiment of the invention, the peptide probes 14 function in the manner described above. The peptide probes act as "nuclei"; wherein once the peptide probe 14 binds to a test sample 20, or a sample known to have beta-rich structure 12, it is converted to a peptide probe conformer 16 which has the capacity to act as a trigger to bind to another peptide probe 14 and continues to induce the same conformational change. Propagation of this reaction can then be controlled by the peptide sequence chosen for the peptide probe 14 and by the experimental conditions. Thus, in situations where infectious levels are low and there is a need to amplify any existing abnormal proteinaceous particles in an unknown sample 20, it is preferred that a peptide probe 14 capable of rapid and continuous propagation of the reaction be chosen with which to nucleate the unknown sample 20. On the other hand, in situations where it is desired to corre-

late detection of abnormally folded proteinaceous particles with levels of infectivity, it is preferred that peptide probe 14 chosen is one that is less likely to aggregate.

When more than one beta units come together, they act as nuclei to attract and stabilize other transient elements of secondary structure. See Stryer, Lubert. *Biochemsitry*. W. H. Freeman Press. (3rd ed. NY 1988) p35. In choosing the peptide probe 14 with which to nucleate this reaction there are several considerations to be made. Associations of peptide can be controlled by the thermodynamics of the solution in which they are in and by the presence of amorphous nuclei which self-associate, crystalline nuclei which readily aggregate, specific peptide sequences which may aggregate, but may do so under low concentrations which are difficult to measure by conventional means, or larger peptide sequences modeled after known beta-sheet structures or proteins such as a beta-rich prion protein.

To demonstrate this embodiment of the invention, two peptide sequences were synthesized to be used as peptide probes 14. The peptide sequences were modeled after known prion protein (PrP) sequences shown in Fig. 13. The sequences in Fig. 13 correspond to binding regions that are very similar among the species shown. Fig. 14 shows the peptide sequences of the two synthesized peptides. The 19-mer sequence referred to as Seq. Id. No. 19 is closely modeled after residues 104 through 122 of the human sequence. The 14-mer sequence referred to as Seq. Id. No. 14 is closely modeled after residues 109 through 122 of the human PrP sequence. The synthetic peptide probes 14 were also prepared with and without pyrene butyric acid as a fluorescence marker.

Many experiments were performed to study the properties of the synthetic peptides. Experiments were performed using analytical techniques common in the art such as absorbance, fluorescence under varying excitation and excitation of fluorescence. The peptides were studied at several concentrations ranging from 1 to 100 micro Molar (µM) and under varying buffer concentrations, pH, temperatures and ionic strengths.

Fig. 15 shows a graph of fluorescence-spectra results at different peptide concentrations. The data were collected over times ranging form one hour to one week with no experimental changes observed after twenty-four hours. The resulting graphs show:

- Sample 46 which was at a concentration of 5 µM with a relative fluorescence peak at approximately 0.1.

- Sample 48 which was at a concentration of 10 µM with a relative fluorescence peak at approximately 0.4.

- Sample .50 which was at a concentration of 150 µM with a relative fluorescence peak at approximately 4.7.

Note: data were also collected for Sample 52 at a high concentration of 800 µM, but is not shown in the figure.

Fig. 16 shows a graph of the fluorescence spectra for samples 46 through 52 normalized to the intensity at 378 nm for the initial scan. It was observed that the spectrum

for Sample 52 which contained the highest peptide concentration was markedly different leading to the conclusion that there is excimer emission with a maximum at approximately 460 nm.

Fig. 17 is a graph of experimental results showing pyrene's excitation of fluorescence. The experiments were performed with excitation wavelengths at 365 nm to observe excimer emission at approximately 460 nm. The excitation at 348 nm, however, increases the fluorescence signal by over a hundred times with no other modifications or signal amplification. To confirm that the pyrene conjugate was responsible for both the major 398 nm emission as well as the one at approximately 460 nm, the excitation spectra for fluorescence at 398 nm and at approximately 460 nm were recorded and are shown in Fig. 18. Both the excitation spectra are nearly identical with a 365 nm maximum confirming that emission at approximately 460 nm is associated with the formation of excimers by two pyrene groups as in the following.

$$Pyr^* + Pyr = (Pyr\_Pyr)^*$$

where Pyr is a pyrene molecule and Pyr* is a pyrene in its excited form; the (Pyr_Pyr)* represents the formation of excited dimer. More general information on excimers can be found in Freifelder, David. *Physical Biochemistry: Applications to Biochemistry and Molecular Biology*, (W. H. Freeman Press, New York, 2nd ed. 1982), at 559.

Experiments were also performed to study the stability of the peptides. Fig. 19 shows experimental data obtained

from circular dichroism (CD) analysis of the 19-mer under different condition. The CD spectra were recorded for a number of peptide concentrations ranging from 20 to 100 mM. The results show that the 19-mer is largely coiled and exhibits high thermodynamic stability under the experimental conditions tested such as varying pH, ionic strength and temperature. As expected, the addition of organics such as acetonitrile and trifluoroethylene (TFE) encourage the formation of the secondary structure. Fig. 20 shows both the previous results and the results of a similar experiment in which the 19-mer was mixed with its shorter analog, the 14-mer. In this experiment, the 19-mer and 14-mer were combined 100:1 for one hour and assembled under dilute conditions in the micro molar range. Sample curves 60 through 64 which correspond to the mixture showed that the mixture of the oligomers significantly differed from the CD spectra of sample curves 52 through 58 which represent the 19-mer alone, indicating strong interactions between the mixed molecules. As a result, the 14-mer triggers conformational changes in a peptide probe 14 made of the 19-mer.

In a paper published by Prusiner, et al., CD data show that the Seq. Id. No. 19, 19-mer exhibits coil-like conformation, whereas the Seq. Id. No. 14, 14-mer is largely beta-sheet as shown in Fig. 21a for a 3 mM concentration sample from the paper. The 19-mer, however, can be transformed from its coil-like conformation to a beta-sheet conformation through interaction with a very small fraction of the 14-mer as shown in Fig. 21b which was tracked over a twenty four hour time period. See Prusiner, *et al. Prion protein peptides induce alph-helix to beta-sheet*

*conformational transitions.* Biochemsitry. 34:4186-92 (1995).

Fig. 22 shows a conceptual figure of the secondary structure of the two synthetic peptides (where C = coil and H =helix) based on the application of various secondary structure algorithms to the sequences of both of the synthetic peptides. The resulting projection, however, does not entirely agree with the CD results. Based on the CD results, the conformations of both synthetic peptides are clearly concentration dependent. Moreover, while the 19-mer exhibits largely a coil conformation that is fairly stable under a wide variety of the experimental conditions tested, the 14-mer exhibits a transition from coil or hairpin to beta-sheet structure depending on its concentration.

More experiments were performed to determine if the 19-mer could self-associate. Fig. 23 shows a graph of fluorescence results showing that the 19-mer could self-associate with increasing concentration as shown in Sample curve 66 and at low concentrations with pH modifications to give a net neutral charge while using potassium chloride (KCl) to screen the charge as shown in Sample curve 68. The 19-mer can also self-associate at low concentrations with the introduction of some type of nucleating agent, as discussed earlier. Thus, the conditions for self-association can be optimized to adapt to a desired type of detection.

The same samples; Sample curve 66 containing 0.1 M TRIS buffer at pH 6 to 9 and Sample curve 68 containing 0.1 M TRIS buffer at pH 10 to 11 in the presence of KCl at 100 to 500 mM, are shown again in Fig. 24 to reflect the efficiency of excimer formation under low concentrations. The ratio of the fluorescence intensities as measured at 378 nm

($I_M$) and at 460 nm ($I_E$) was chosen to monitor the self-association as a function of the peptide concentration at 25°C. It was also shown that screening of the electrostatic interactions (pI = 10) encouraged self-association at extremely low concentrations on the order of less than 10 micro Molar.

In order to further study the effect of nuclei on the self-association of the 19-mer, more fluorescence measurements were taken of 19-mer in solution nucleating with small amounts of already self-associated 19-mer units. The sample solutions range from concentrations of 200 to 800 micro Molar and are described in Fig. 25. The kinetics of association in dilute solutions of 20 micro Molar were also monitored.

Fig. 26a shows more fluorescence data of the 19-mer in water 70, acetonitrile 72 and TFE 74 after twenty-four hours. Fig. 26b shows the experimental results for a 100:1 combination of the 19-mer and 14-mer in water 76, acetonitrile 78 and TFE 80 after twenty-four hours. In both of the graphs in Fig. 26 peptide association was monitored by the appearance of excimer emission at approximately 460 nm.

Figs. 27 a, b, c, and d show four fluorescence data graphs taken at 24, 48, 144 and 336 hours, respectively. The measurements were taken to determine the effect of pH, temperature, ionic strength, and organic additives on the kinetics of the peptide associations studied for the 19-mer model peptide. The fluorescence intensities as measured at 378 nm for monomeric units and 460 nm for associations were used to characterize the $I_E/I_M$ ratio or self-association of the peptide.

Additional fluorescence results are shown in Fig. 28 where an insoluble fraction of the peptide was extracted

and dissolved in organic solvent containing methanol /ethanol/ dimethylformanide and then analyzed. Fluorescence detection results of the "insoluble" portion show high levels of peptide association wherein the $I_E/I_M$ ratio equals 2. A small aliquot of "insoluble" portion was added to nucleate 20 micro Molar 19-mer peptide solutions which were then analyzed and are reported in the same graph. The results show that the presence of the nucleating fraction significantly increased the efficiency of the peptide association and this can be seen more dramatically in Fig. 28b at 150 hours.

The observations of these experiments led to some of the following conclusions.

- Fluorescence of pyrene, which is covalently attached to the peptide probe 14 in preferred embodiments, allows monitoring of peptide self-association in this model system. It can also be used as an index of conformational change and especially since at low concentrations, the peptide association is difficult to measure using nonoptical techniques.

- The fluorescence data shows that self-association of the Seq. Id. No. 19, 19-mer, can be promoted by adjusting ionic strength or pH.

- The fluorescence data also shows that the kinetics of the conformational changes can be modulated by controlling solvent parameters and the peptide probe sequence.

- The kinetics of the self-assembly or association process can be controlled or regulated by the addition of or by preexisting nucleating associated forms. This strongly supports the conclusions that the conformational transitions of the 19-mer can be autocatalytic.

In a particularly preferred embodiment, the peptide probes 14 can be used to detect proteinaceous particles such as in prion-like structures exhibiting coil to beta-sheet transition. According to Prusiner, *et al. Prion protein peptides induce alph-helix to beta-sheet conformational transitions. Biochemsitry.* 34:4186-92 (1995). As a result, synthetic peptide probes such as the Seq. Id. No. 19, 19-mer should be conformationally sensitive to the presence of prion-like substances that undergo this conformational shift. Moreover, because an intrinsic optical reporter, such as pyrene can be added to the peptide probe, this embodiment of the invention has the added advantage of being able to detect such prion-like substances in test samples 20 such as blood, lymph, CSF and even tissues other than brain homogenate that typically contain very low levels of abnormal prion substances that are otherwise too difficult to detect. The intrinsic optical reporter allows optical (fluorescence) measurements to be taken of the peptide probe associates that form upon interaction with nucleating samples such as an abnormal prion.

In another particularly preferred embodiment of the invention, the peptide probes 14 are synthesized based on

the structure of a dendrimer; dendrimers being synthesized three-dimensional highly branched macromolecules. The advantages of using a dendrimer probe 15 are multifold. Dendrimers should increase the speed of the assay kinetics thereby relaying quicker test results. This can be especially advantageous in assembly line applications of the invention where products or specimens in mass quantities can be quickly tested for the presence of abnormal proteinaceous particles. This embodiment is also extremely beneficial in applications where quick decisions must be based on the detection results. This embodiment is also advantageous for use in these applications as well as others since the highly branched structure of the dendrimer prevents amplification of abnormal proteinaceous particles or aggregates. By preventing such amplification of the abnormal particles, it becomes very simple to correlate the detection results with the level of abnormal aggregates existing in a test sample 20. Furthermore, it is also safe to handle since the synthetic probe itself is nonneurotoxic and amplifies signal without amplification of any highly infectious particles that may be preexisting in a test sample 20. Thus, it eliminates the need for extra precautions or sterilization in many of the steps of the assay method.

A generalized dendrimer 15 structure is shown in Fig. 29 and is referred to as Seq. Id. No. 20. In a particularly preferred embodiment of the invention, a specific dendrimer structure was designed and synthesized, referred to as Seq. Id. No. 22 and is shown in Fig. 30.

In Fig. 30, the specific dendrimer structure is basically a loop-turn-loop structure as illustrated by Fig. 30a. In Fig. 30b, it is shown that the sequence is modeled

after the human PrP sequence shown in Fig. 14 in residues 126 through 104 plus 109 through 126. This structure shows the region on the right 74 as an inverted form of the PrP sequence. This was done to take advantage of the five aminoacids which naturally form a loop in order to place hydrophobic pyrene in a corresponding hydrophobic region. Also the valine-valine fragment is essential to beta-sheet formation and so is retained in the sequence. In the figure, green denotes possible mouse variants. The amyloidogenic palindrome region 70 may be changed to SS or SSS/AAA. The central region 72 is a loop sequence with steric constraints, thus it is possible to add tryptophan for steric and fluorescence considerations.

Modifications of the aminoacid sequence such as one or more deletions or insertions are possible as alluded to above, provided that the dendrimer retains its branched loop-turn-loop structure as well as aminoacids essential to beta-sheet formation, and preferably contains an optical reporter.

Fig. 10 shows a schematic diagram of how the dendrimer probes 15 amplify signal and propagate conformational change without aggregation and without increasing the biohazard or infectious nature of an abnormal protein or prion test sample 12. The figure shows that once the dendrimer probes 15 come into contact with the abnormal sample 12, the dendrimer probe 15 undergoes the conformational shift to a predominately beta-sheet structure 17. The newly formed beta-rich dendrimer probe 17 nucleates other dendrimer probes 15 to make the same transition. By doing so, any optical signal associated with the dendrimer probe 15 is amplified as more probes 15 shift to the beta-rich state 17.

It is important to note that the minimal detectable concentration of pyrene only provides a number for the peptide probe 14 concentration that can be worked with; but the detection limit of the assay is not dependent on it because it is the resultant of the fluorescent ensemble that is being observed. In other words, the real measurement of interest and the rate limiting step in the analysis is the amount of abnormal e. g. prion protein that need to be present in the sample 20 to initiate a conformer change in the peptide probe 14. Immunoassays are typically sensitive in the picomolar range. Nevertheless, once the conformer change is initiated in a single peptide probe 14, the catalytic propagation of its beta-rich structure allows detection in samples previously considered to have abnormal particles 12 at concentrations too low to detect.

Due to its ability to safely, quickly and noninvasively detect abnormal proteinaceous particles such as misfolded proteins, prions, aggregates and fibrils that may lead to toxic plaque formations, the method of this invention is widely applicable to many industries. By example, some of those industries include the diagnostics markets in animal health and human health, the food industry, pharmaceutics, especially for screening animal by-products, transplant/transfusion and vaccine supplies, research and development in such areas as chemotherapies for TSE's, as well as national security in the area of biosensors for biowarfare agents.

Accordingly, in yet another preferred embodiment of the invention, the methods discussed herein can be applied for use with a simple detection instrument such as the one shown in Fig. 31. The device shown in Fig. 31 is a simple

optical device that includes a light source 80 shown in blue *e. g.* lamp or laser; a T-format sample cell 82 shown in grey; and a photomultiplier tube 84 shown in pink. In certain applications it may be desirable to have the method distributed as an assay that includes such a simple device.

Accordingly, the present invention is not limited to the specific embodiments illustrated herein. Those skilled in the art will recognize, or be able to ascertain that the embodiments identified herein and equivalents thereof require no more than routine experimentation, all of which are intended to be encompassed by claims.

Furthermore, it will be understood that the foregoing disclosure is intended to be merely exemplary, and not to limit the scope of the invention -- which is to be determined by reference to the appended claims.

WHAT IS CLAIMED IS:

1. A method for rapid preclinical detection of infectious conformationally altered proteins; said method comprising:

obtaining a test specimen;

adding a propagation catalyst to the specimen;

allowing the catalyst and the specimen to interact forming a mixture; and

observing any increase in beta-sheet formation in the mixture.

2. The method of claim 1, wherein:

said obtaining step does not include physically sacrificing a subject from which the test specimen is obtained.

3. The method of claim 1, wherein:

said obtaining step is noninvasive in that it encompasses drawing body fluids but does not encompass biopsy of tissues or organs.

4. The method of claim 1, wherein:

said propagation catalyst is an agent which undergoes a conformational shift toward beta-sheet formation upon contact with a proteinaceous particle.

5. The method of claim 4, wherein:
said propagation catalyst is an optical labeled peptide.

6. The method of claim 4, wherein:
said peptide is a peptide having the amino acid seqence of Seq. Id. No. 19.

7. The method of claim 1, wherein:
said propagation catalyst is a dendrimer.

8. The method of claim 7, wherein:
said dendrimer is a dendrimer having the amino acid seqence of Seq. Id. No. 20.

9. The method of claim 7, wherein:
said dendrimer is a dendrimer having the amino acid seqence of Seq. Id. No. 22.

10. The method of claim 4, wherein:
said proteinaceous particle is a predominately beta-sheet structure.

11. The method of claim 4, wherein:
said proteinaceous particle is a $PrP^{sc}$ particle.

12. The method of claim 1, wherein:
addition of said propagation catalyst to a test specimen containing selected abnormal proteinaceous particles increases beta-sheet formation of the propagation catalyst.

13. The method of claim 1, wherein:
addition of said propagation catalyst to a test specimen containing $PrP^{SC}$ increases beta-sheet formation of the propagation catalyst.

14. The method of claim 1, wherein:
said propagation catalyst is an abnormal proteinaceous particle ($PrP^{SC}$).

15. The method of claim 10, wherein:
addition of said propagation catalyst to a test specimen containing proteinaceous particles of substantially only a PrPSc type cause an increase in beta-sheet formation of the mixture.

16. The method of claim 1, further comprising:
designation of a test subject requiring therapeutic treatment based on the detection of infectiously conformationally altered protein in the sample taken from such test subject.

17. The method of claim 1, wherein:
the test subject is a human being.

18. The method of claim 1, wherein the steps of obtaining and observing involve receiving and monitoring of products from the group consisting of:
health research, pharmaceuticals, food industry and biosensors for national security.

19. The method of claim 1, method of claim 1, wherein the steps of observing involve monitoring of products from the group consisting of:
animal by-products, chemotherapies, transplant, transfusion and vaccine supples.

20. A method for using a device for rapid preclinical detection of infectious conformationally altered proteins, wherein said device comprises:
a light source;
a flow cell; and
a photomultiplier.

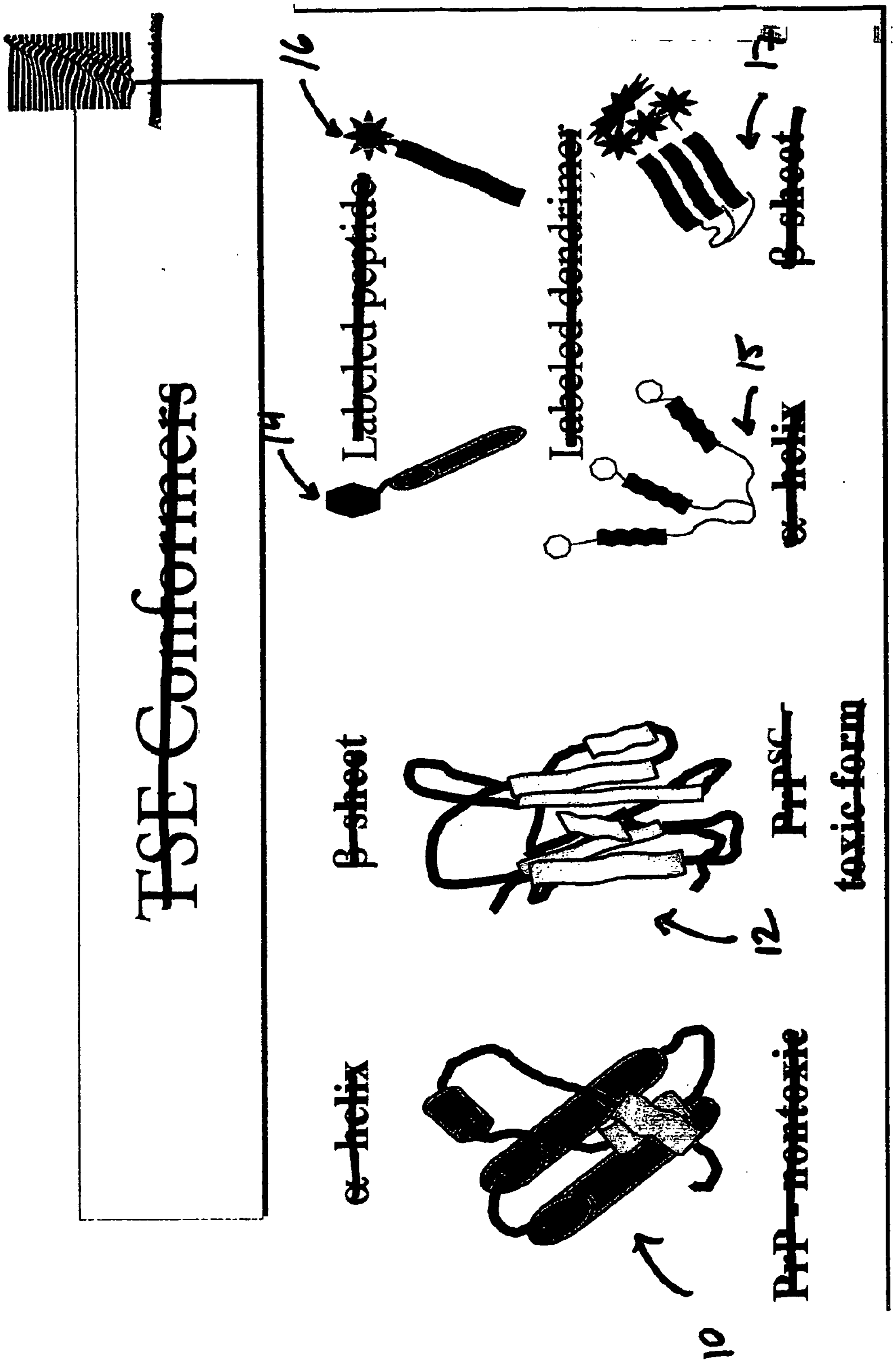


Figure 1

~~Private & Privileged Information~~

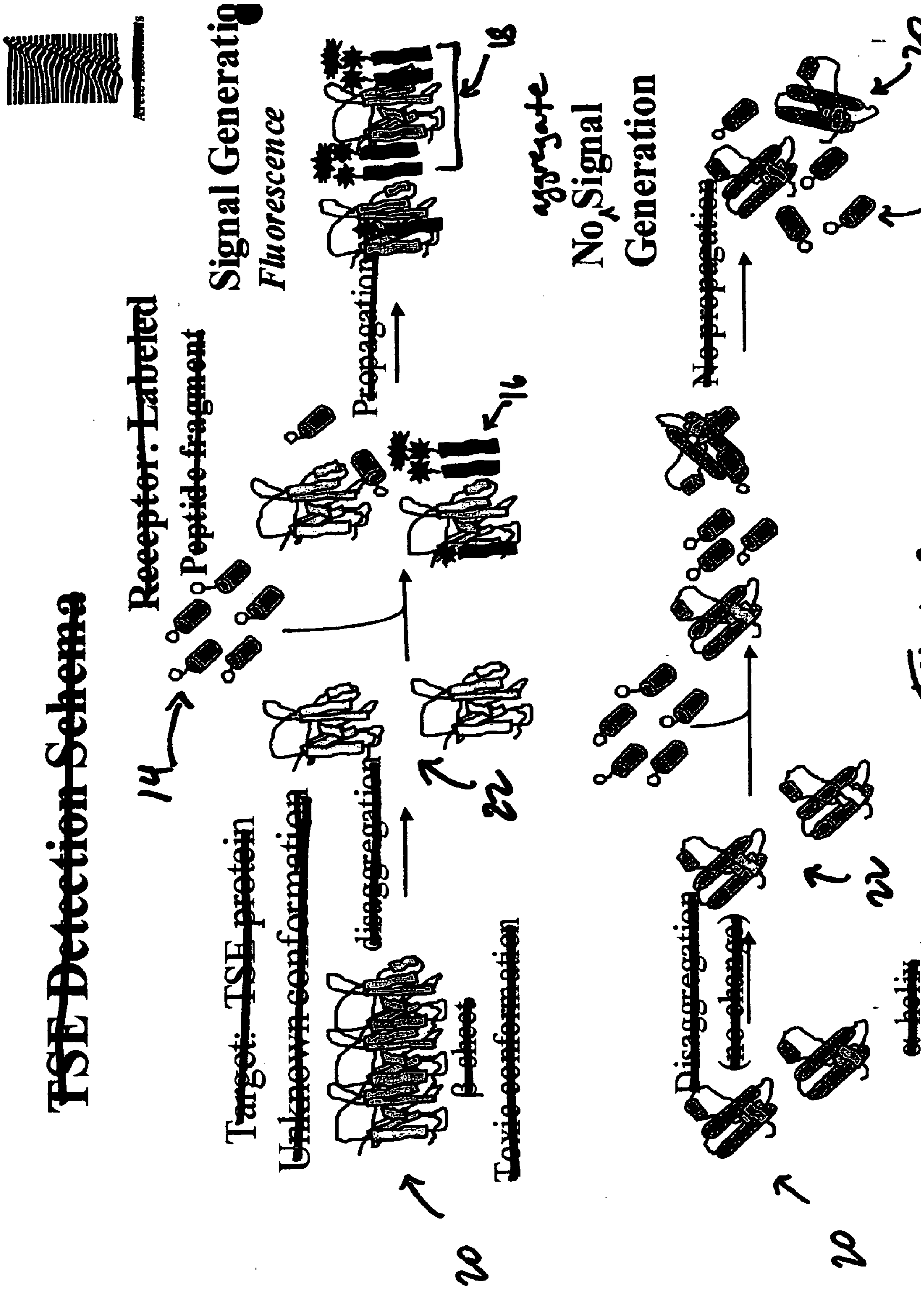
TSE Detection Schema
Target: TSE protein
Unknown conformation
β-sheet
Toxic conformation
disaggregation
14
22
20
Receptor: Labeled
Peptide fragment
16
Propagation
Signal Generatio
Fluorescence
18
No aggregate Signal
Generation
No propagation
Disaggregation
(no change)
α-helix
22
20

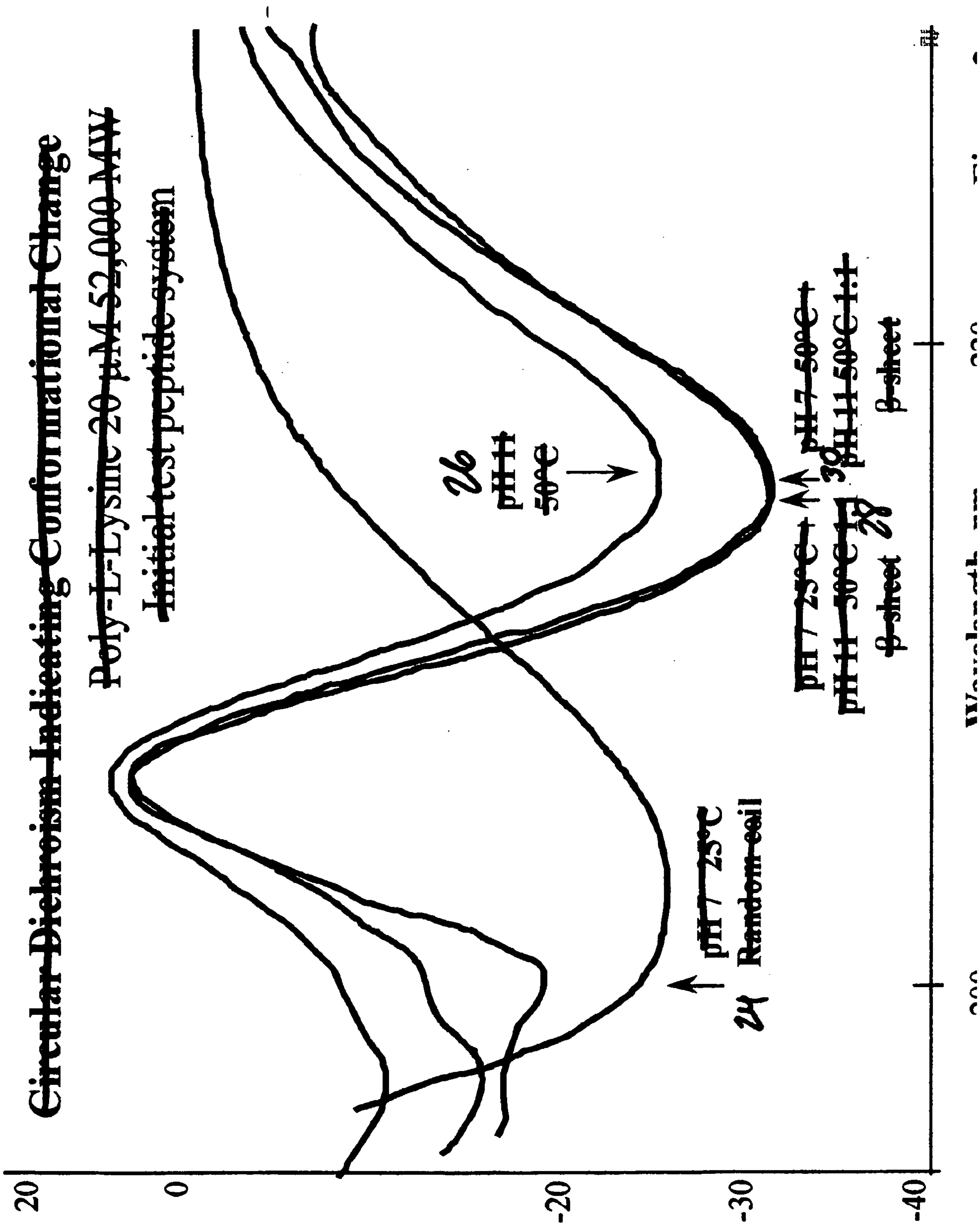
~~Circular Dichroism Indicating Conformational Change~~
~~Poly-L-Lysine 20 μM 52,000 MW~~
~~Initial test peptide system~~
~~pH 7 25°C~~
~~Random coil~~
24
26
~~pH 11~~
~~50°C~~
~~pH 7 25°C~~
~~pH 11 50°C 1:1~~
~~β-sheet~~
28
30
~~pH 7 50°C~~
~~pH 11 50°C 1:1~~
~~β-sheet~~
20
0
-20
-30
-40

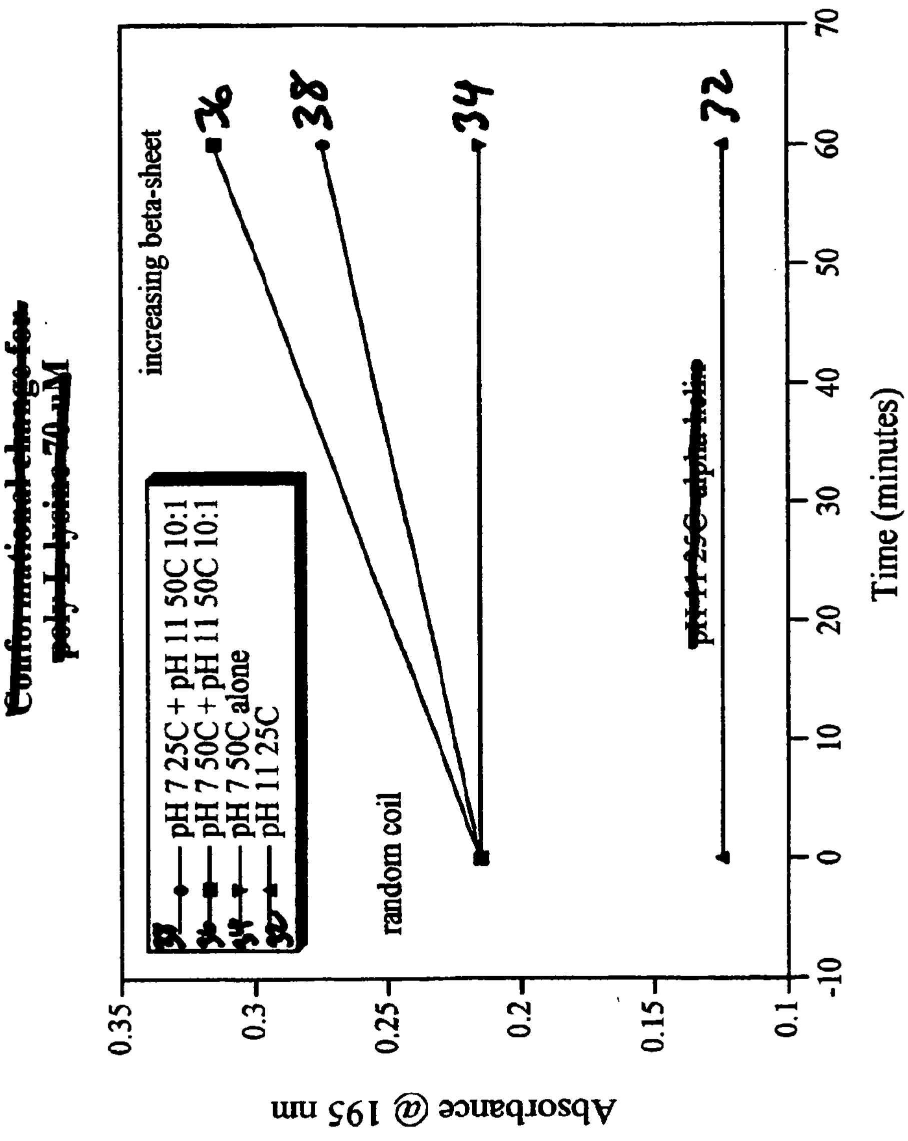
~~Conformational change for poly-L-lysine 70 uM~~
increasing beta-sheet
random coil
~~pH 11 25C alpha-helix~~
38 — pH 7 25C + pH 11 50C 10:1
36 — pH 7 50C + pH 11 50C 10:1
34 — pH 7 50C alone
32 — pH 11 25C
36
38
34
32
Absorbance @ 195 nm
0.35
0.3
0.25
0.2
0.15
0.1
-10
0
10
20
30
40
50
60
70
Time (minutes)

Figure 4

| Temperature (°C) | 25 °C | 50 °C |
|---|---|---|
| pH 7 alone | Random coil | Random coil |
| pH 11 alone | alpha-helix | beta-sheet |
| pH 7 + pH 11 | beta-sheet | beta-sheet |
| pH 11 at 25 °C + pH 11 at 50 °C | Random coil | ----------- |

**Figure 5**

~~The data are from previous experiments for proximal and distal locations in an α-helical bundle structure undergoing conformational change.~~

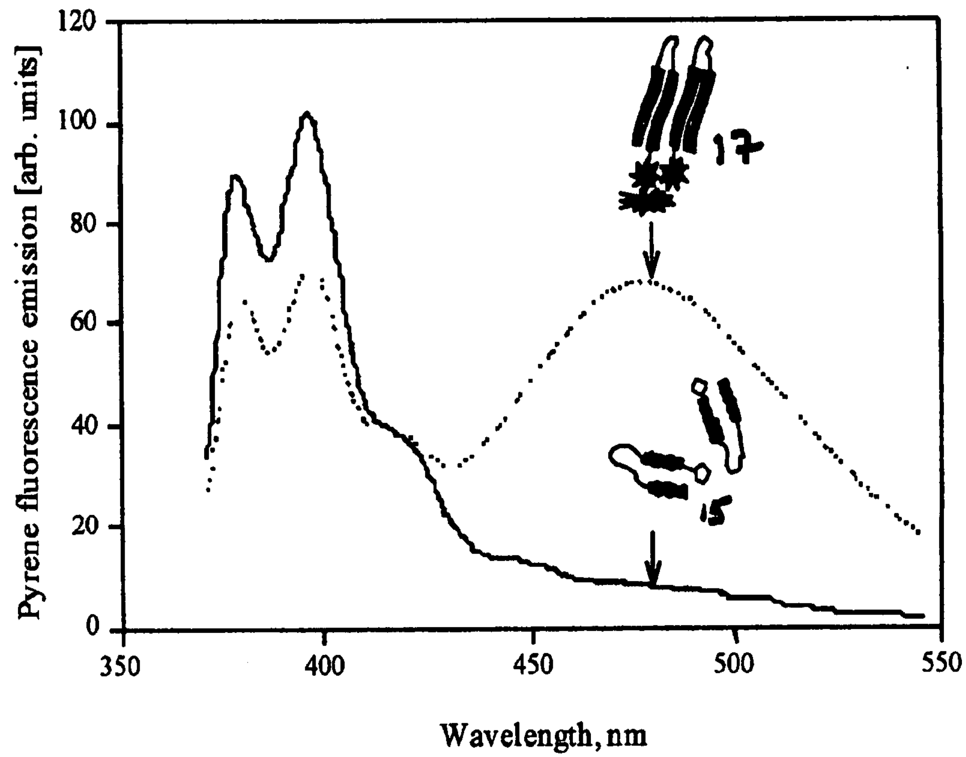


Figure 6

~~The spectra shown are for pyrene excimer formation at 480 nm, but other probes can be used.~~

## ~~Engineering considerations for sensor design~~

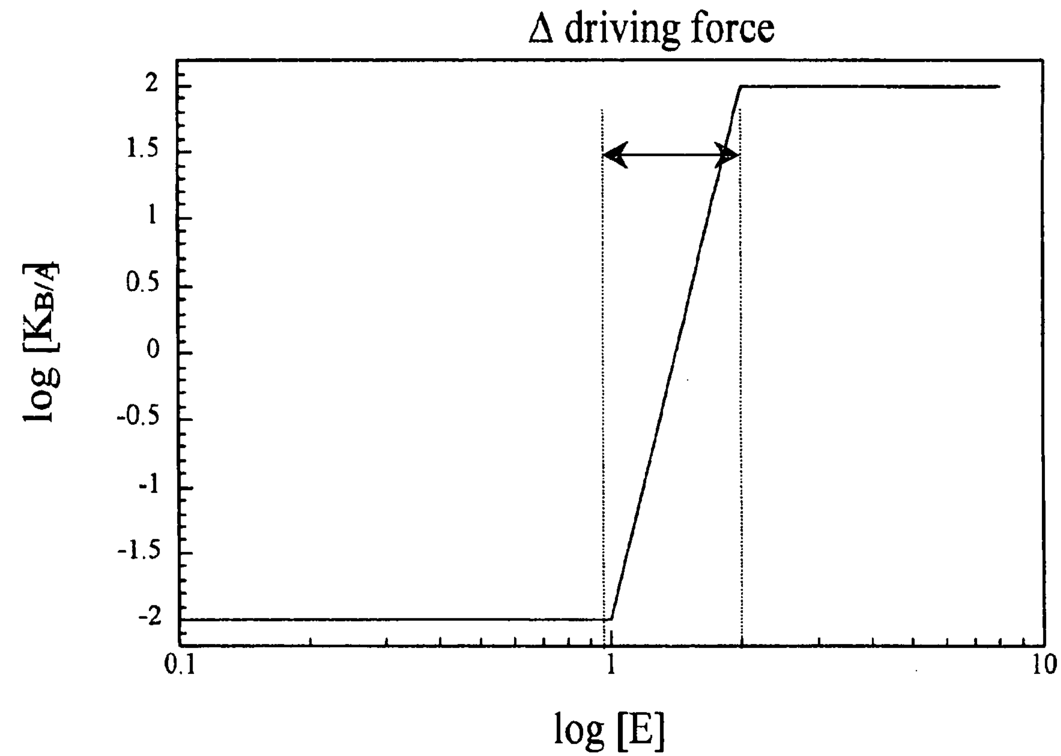


~~The driving force must be commensurate with the energetic difference between the two conformational states~~

~~The process is driven by a differential interaction of the target peptide E, with the two conformations of the test PrP molecule.~~

Figure 7

# ~~Overview of Prions~~

Fig. 8

- ~~Transmissible Spongiform Encephalopathies (TSEs)~~
  - ~~Scrapies~~
  - ~~Mad Cow (BSE)~~
  - ~~Creutzfeldt-Jakob Disease (CJD)~~
  - ~~Chronic Wasting Disease (CWD)~~
  - ~~nvCJD~~
- ~~"*folding diseases*": characterized by proteins with destabilizing conformers which tend to aggregate and form toxic plaques in brain tissue~~

~~Normal PrP Protein~~

- ~~a cell-surface metallo-glycoprotein~~
- ~~mostly α-helix and loop structure~~
- ~~sensitive to proteases~~
- ~~expressed in the CNS and lymphatic~~

~~Proposed Function~~

- ~~anti-oxidant role~~
- ~~cellular homeostasis~~

~~Disease Process~~

- ~~resistant to proteases~~
- ~~mostly β-structure~~

~~What goes wrong?~~

- ~~Conformational change leads to aggregation, neurotoxic fibril formation and plaque deposition~~

~~Private & Privileged Information~~ Fig. 9 10

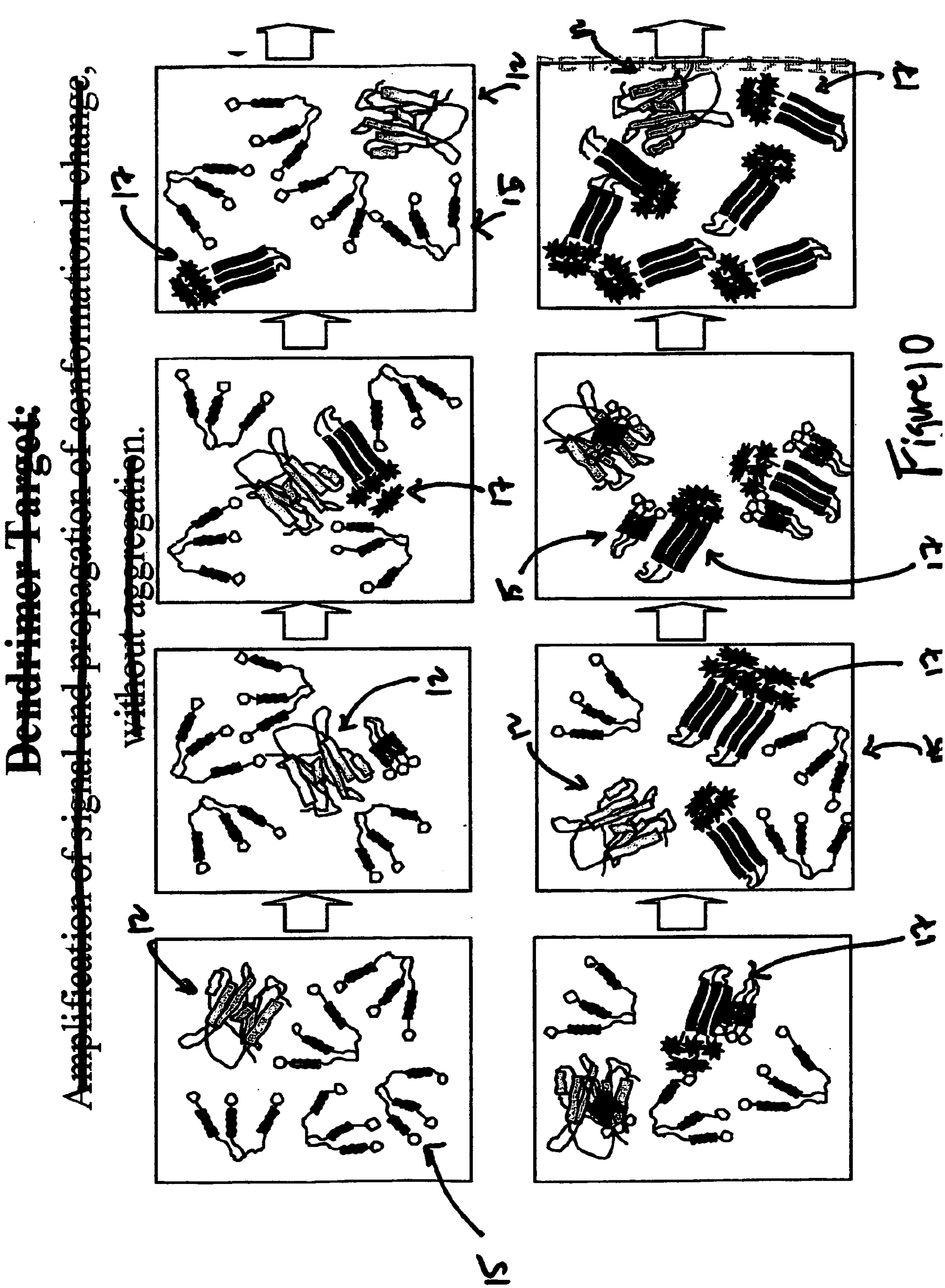
~~Dendrimer Target:~~
~~Amplification of signal and propagation of conformational change, without aggregation.~~

Figure 10

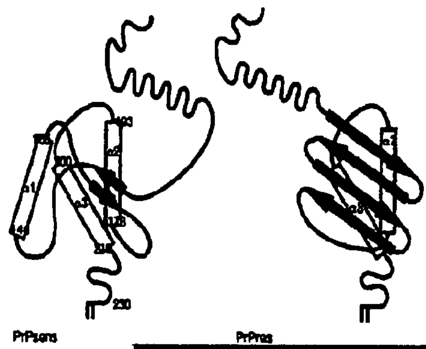


# ~~Current Prion-Diagnostic Market Competition~~

Figure 11

- ~~Three European Union certified tests from:~~
  - ~~Prionics (Swiss): Western blot uses monoclonal antibody to detect PrP in brain tissue from dead animals in 7 to 8 hours~~
  - ~~Enfer Scientific (Irish): ELISA based, testing on spinal cord tissue from dead animals in under 4 hours~~
  - ~~CEA (French): sandwich immunoassay using two monoclonals on brain tissue collected after death in under 24 hours~~

# EU Test Results

| Tests Evaluated | Sensitivity *true positive* | Specificity *true negative* | Detection Limit*^ |
|---|---|---|---|
| Prionics Check | 100% | 100% | $10^{-1}$ ~126 LD50/g |
| Enfer | 100% | 100% | $10^{-1.5}$ ~70 LD50/g |
| CEA | 100% | 100% | $10^{-2.5}$ ~7 LD50/g |
| E.G. & G. Wallac | 70% | 90% | $10^{0}$ ~1259 LD50/g |

* Material used to prepare dilutions was bovine nervous tissue titrated in mice at $10^{3.1}$ mouse i.c. LD50/g of tissue. (= 1259 LD50/g)

^ An infectious dose is designated to be $10^5$ PrP monomers per Brown *et al.* (1994) Ann. Neurology 35:513-529

~~Private & Privileged Information~~

Figure 12

~~Selected PRP Sequence~~
~~Species Comparison~~

| | 104 | 110 | 120 | 130 | 140 | |
|---|---|---|---|---|---|---|
| *Human* | KPKTNMKH | MAGAAAAGAVVGGLGGY | MLGSAMSRP | I I | HF | |
| *Hamster* | KPKTNMKH | MAGAAAAGAVVGGLGGY | MLGSAMSRP | MM | HF | |
| *Mouse* | KPKTNLK H | VAGAAAAGAVVGGLGGY | LGSAMSRP | M I | HF | |
| *Bovine* | KPKTNMKH | VAGAAAAGAVVGGLGGY | LGSAMSRP | P I | HF | |
| *Elk* | KPKTNMKH | VAGAAAAGAVVGGLGGY | LGSAMSRP | L I | HF | |
| *Deer* | KPKTNMKH | VAGAAAAGAVVGGLGGY | LGSAMSRP | L I | HF | |

Figure 13

19-mer *KPKTNMKHMAGAAAAGAVV Seq. Id. No. 19
14-mer *MKHMAGAAAAGAVV Seq. Id. No. 14.
lys-pro-lys-thr-asn-met-lys-his-met-ala-gly-ala-ala-ala-ala-gly-ala-val-val
(—With and without the conjugate *pyrene butyric acid)

Figure 14

~~Private & Privileged Information~~ ~~22~~

# ~~Peptide Concentration Effect~~

- ~~Fluorescence spectra recorded for 5, 10 and 150 uM (from bottom to top) are shown as an example of the effect of increasing peptide conc. The highest conc. at 800 uM is not in view.~~

- ~~Data were collected over time from 1 h to a week with no experimental changes observed after 24 h.~~

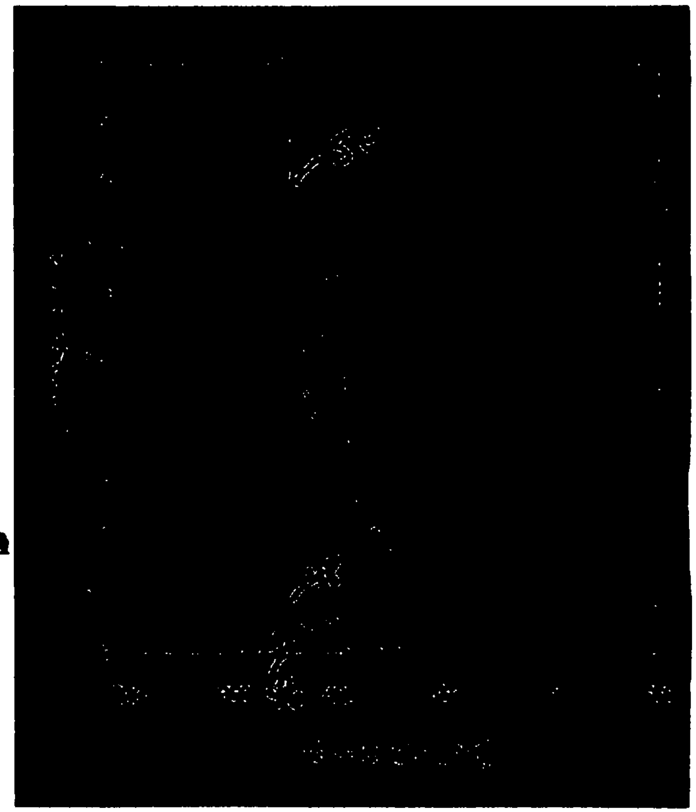

~~Private & Privileged Information~~ Figure 15

# ~~Fluorescence Study Finding~~

- ~~Fluorescence spectra normalized to the intensity at 378 nm for the initial scan were collected for the four uM peptide concentrations: 5 (1), 10 (2), 150 (3) and 800 (4)~~

- ~~Spectrum for the highest peptide concentration, 800 uM(4), is different, and the suspected *excimer emission with maximum at ~460 nm* can be observed.~~

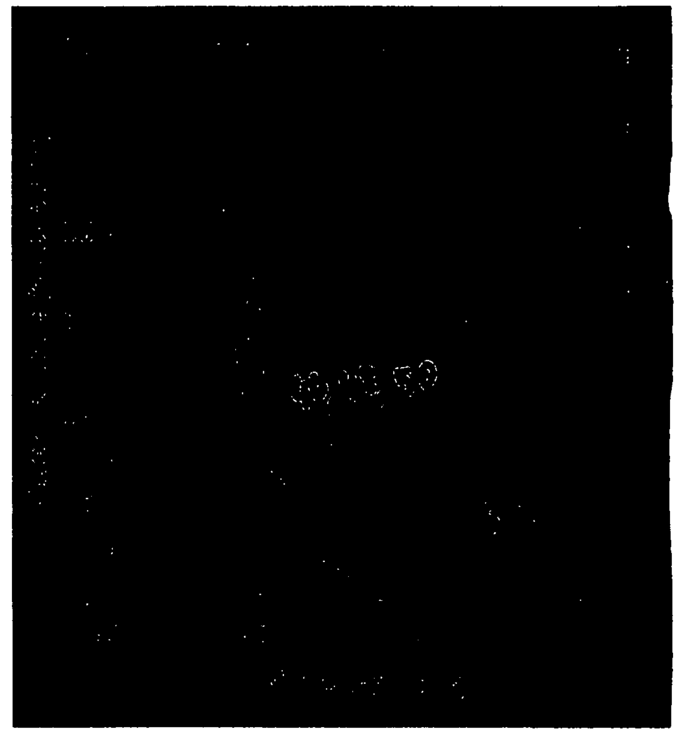

~~Private & Privileged Information~~ Figure 16

# ~~Pyrene's Excitation of Fluorescence~~

- ~~The excitation of fluorescence for the labeled peptide provides encouraging evidence.~~
- ~~Current experiments were performed with the excitation wavelength at 365 nm to see excimer emission at ~460nm.~~
- ~~However, excitation at 348 nm increases the fluorescence signal by over 100 times with no other modifications or signal amplification.~~

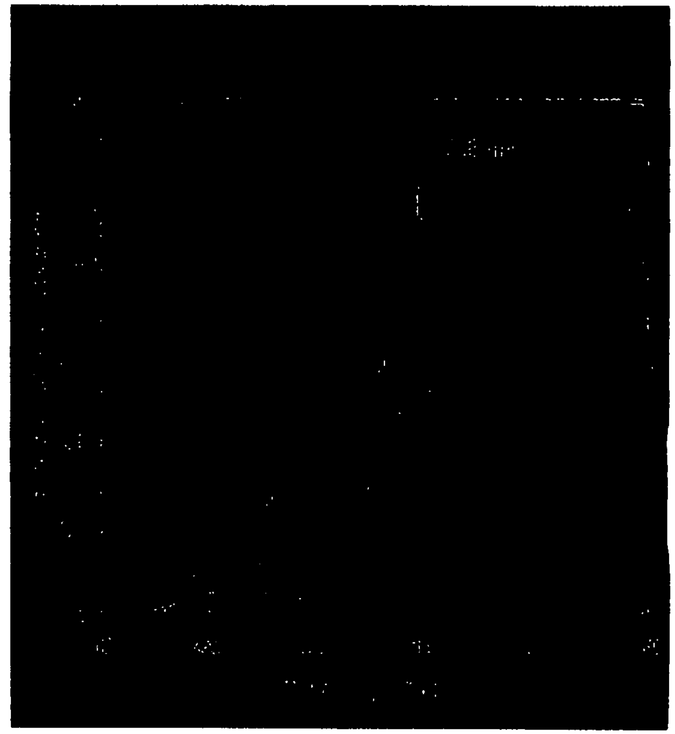

~~Private & Privileged Information~~ Figure 17

# ~~Excitation Spectra for Fluorescence~~

- ~~To confirm that the pyrene conjugate was responsible for both the major 398 nm emission as well as the one at ~460 nm, the excitation spectra for fluorescence at 398 nm and at ~460 nm were recorded.~~
- ~~Both excitation spectra are nearly identical with a 365 nm maximum confirming that emission at ~460 nm is associated with the formation of excimers by two pyrene groups.~~
- Pyr * + Pyr = (Pyr_Pyr)*

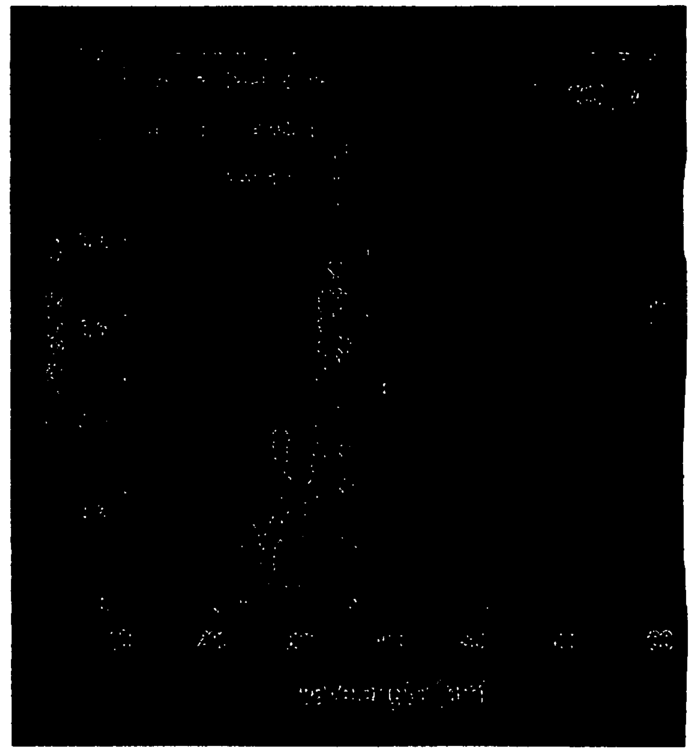

Figure 18

~~Private & Privileged Information~~

# ~~Peptide Stability~~

- ~~Circular dichroism spectra were recorded for a number of peptide concentrations ranging from 20 - 100 uM~~
- ~~CD data show that the 19-mer is largely coiled and exhibits high thermodynamic stability under experimental conditions tested (pH, ionic strength, T°, etc)~~
- ~~As expected, the addition the organic additions (acetonitrile, TFE) encouraged the formation of the secondary structure~~

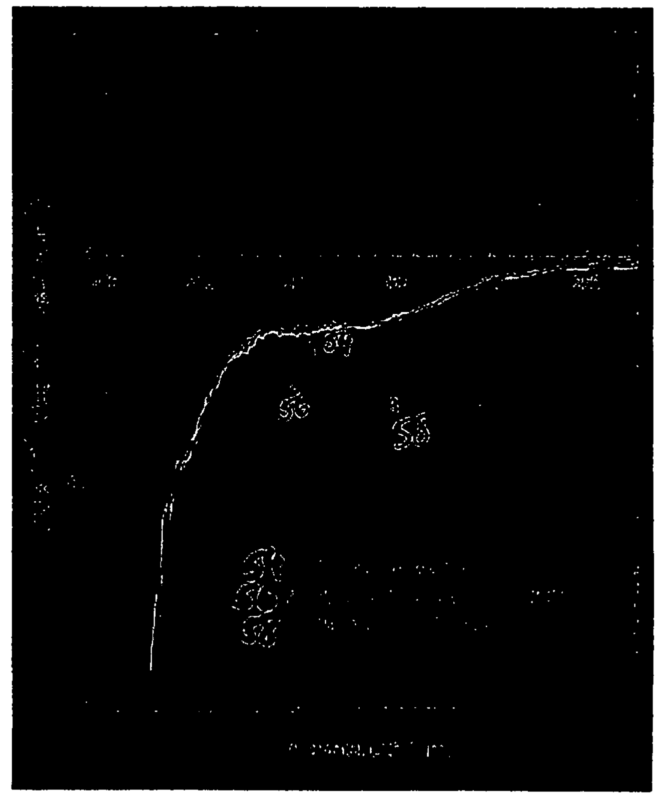

~~Private & Privileged Information~~

Figure 19

Associates

# ~~Interaction with Short Analog~~
# ~~Circular Dichroism~~

- ~~CD spectra were recorded for mixtures of the target peptide (19-mer) and its shorter analog (14-mer).~~
- ~~Addition of the 14-mer (curves 4-6) significantly change the CD spectra of the 19-mer (curves 1-3) indicating strong interactions between these molecules.~~
- ~~The 14-mer triggers conformational changes in the target peptide. Assembling of the peptide fragments occurred under dilute conditions (μM).~~

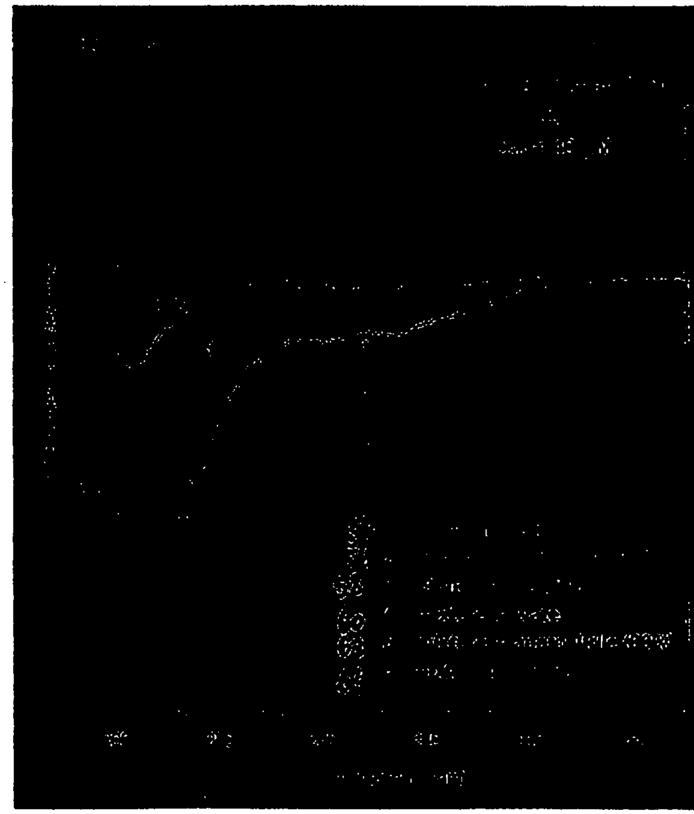

~~Private & Privileged Information~~

Figure 20

~~20~~

# ~~Conformational Lability of Peptide~~

- In ~~good agreement with previous results, it has been shown that the 19-mer exhibits coil-like conformation, whereas the 14-mer is largely β-sheet~~.

- It ~~has also been shown that the 19-mer can be transformed from the coil-like conformation to a β-sheet conformer through interaction with very small fraction of the 14-mer.~~

a

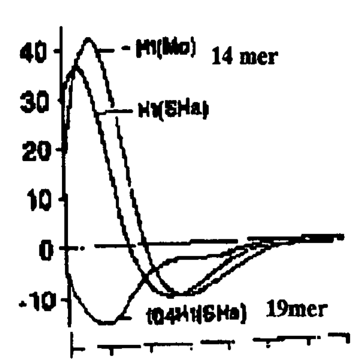


~~The 14-mer assumes a β-sheet conformer while the 19-mer remains in a coiled conformer alone 3 mM.~~

b

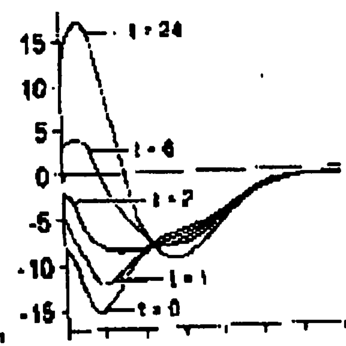


~~Addition of the 14 mer to 19 initiates a phase shift to β-sheet over a 24 h time period~~

Nguyen J, Baldwin MA, Cohen FE, Prusiner SB (1995) Prion protein peptides induce alpha-helix to beta-sheet conformational transitions. Biochemistry 34:4186-92.

~~Private & Privileged Information~~

Figure 21

# ~~Summary of CD Experiments~~

- ~~Various secondary structure algorithms were applied to the primary sequences of both peptides. Theoretical secondary structure predictions simulated for 14- and 19-mers show a significant tendency to adopt a partial α-helical conformation~~:

[redacted] Seq Id. No. 19

Seq Id. No. 14

- ~~This, however, does not agree with the CD data.~~
  - –~~Conformation of both peptides are clearly concentration dependent~~
  - –~~19-mer exhibits largely a coil conformation, which is stable under a wide variation of the experimental conditions (current results)~~.
  - –~~14-mer exhibits a transition from coil or hairpin to β-sheet structure depending on concentration.~~
- ~~The 19-mer should be conformationally sensitive to the presence of prion-like structures exhibiting 'coil - β -sheet transition~~'.

21

Figure 22

Arctos Associates

# ~~Does the peptide self associate?~~

- ~~Can this peptide self associate?~~
  - ~~Yes, with increasing concentration (Curve 1)~~
  - ~~At low concentrations with pH modification to give a net neutral charge and using KCl to screen charge (Curve 2)~~
  - ~~Also at low concentrations with the introduction of "nuclei" acting as a seed or initiator (later charts).~~
- ~~We can optimize the conditions for peptide self association.~~

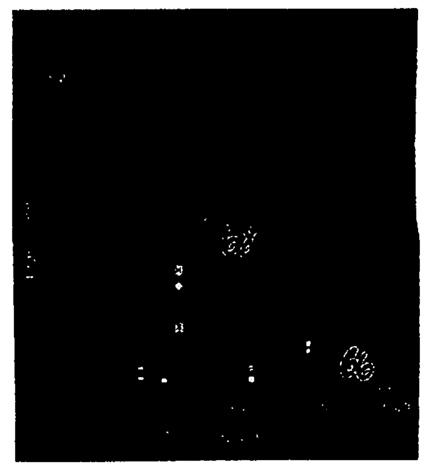

~~Private & Privileged Information~~

Figure 23

# ~~Efficiency of Excimer Formation~~

## ~~*under low concentrations*~~

- ~~The ratio of fluorescence intensities as measured at 378 nm ($I_M$) and at 460 nm ($I_E$) was chosen to monitor the self association as a function of peptide concentration at 25 °C~~:
- ~~Curve 1 - 0.1 M TRIS, pH 6-8;~~
- ~~Curve 2 - 0.1 M TRIS, pH 10-11 in the presence of KCl (100-500 mM)~~.
- ~~Screening of the electrostatic interactions (pI ~ 10) encourage~~s ~~self association at extremely low concentration (< 10 μM).~~

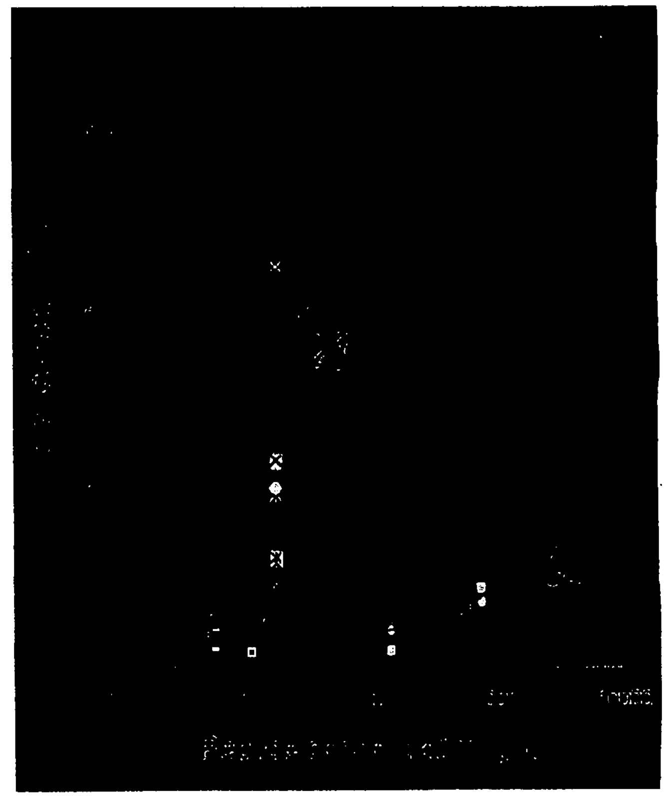

~~Private & Privileged Information~~

Figure 24

# ~~Catalytic Conformational Transition~~ - ~~Effect of Nuclei on Self-Association~~

- ~~Peptide stock solutions of 200 and 800 µM (without and with associates, inset) were~~

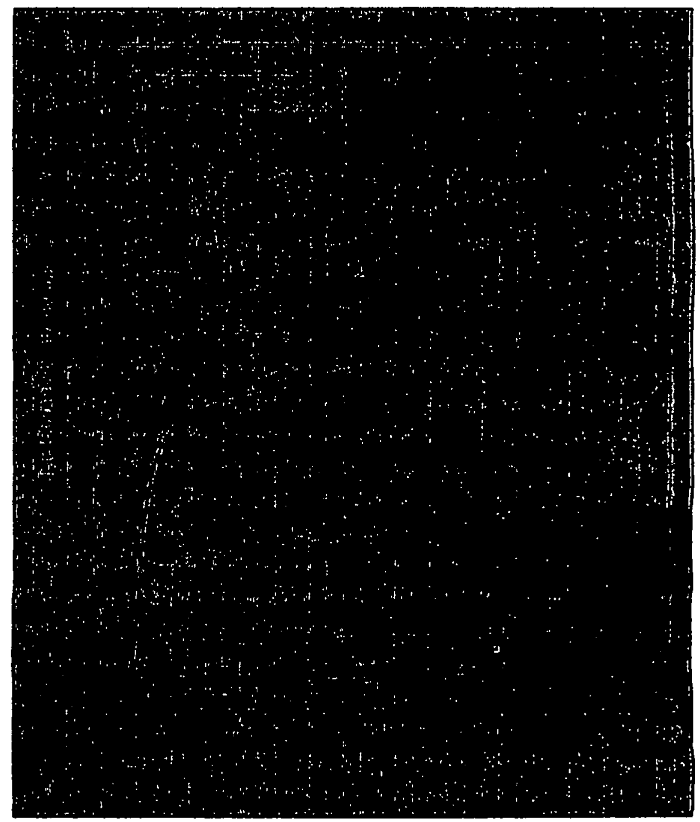

—○— 0.1 M TRIS pH 10
—□— 0.1 M TRIS pH 10, 150 mM KCl
—△— 0.1 M TRIS pH 10, 500 mM KCl
—■— 0.1 M TRIS pH 8, 300 mM KCl
—▲— 0.1 M TRIS pH 8, 500 mM KCl
—●— 0.1 M TRIS pH 10, 15 % acetonitrile
—■— 0.1 M TRIS pH 10, 30 % acetonitrile
—▲— 0.1 M TRIS pH 10, 15 % acetonitrile, 300 mM KCl
—◆— 0.1 M TRIS pH 10, 30 % acetonitrile, 300 mM KCl
—●— 0.1 M TRIS pH 10, 10 % TFE
—■— 0.1 M TRIS pH 10, 20 % TFE
—▲— 0.1 M TRIS pH 10, 10 % TFE, 300 mM KCl
—◆— 0.1 M TRIS pH 10, 20 % TFE, 300 mM KCl

~~Privileged Information~~

Figure 25

34

# ~~Interaction with Short Analog~~g ~~Fluorescenc~~e

- S~~mall additions o~~f ~~the 14 mer pepti~~de ~~significan~~tly e~~ncouraged the~~ ~~self assembling o~~f ~~the 19 mer target~~ ~~peptide~~.
- ~~Association was monitored by the appearance of the excimer emission a~~t ~~460 nm~~.

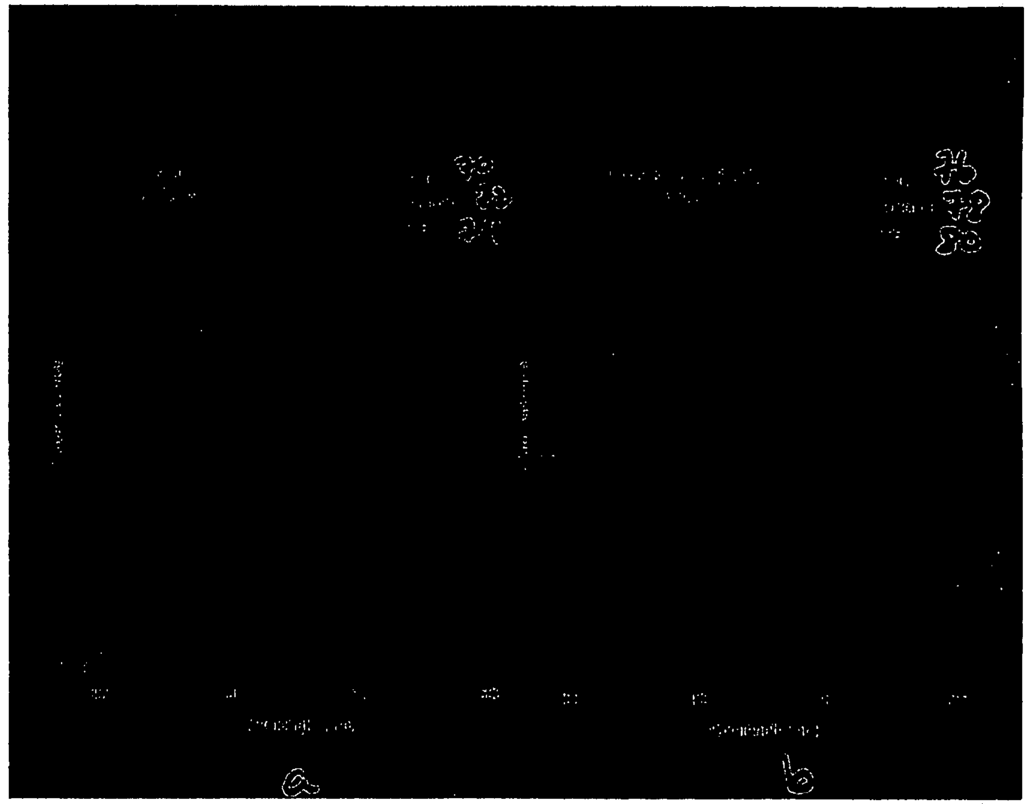


~~Private & Privileged Information~~ Figure 26 ~~26~~

# ~~Effect of Nuclei on Self-Association~~
# ~~RAW DATA~~

- ~~Effect of pH, temperature, ionic strength, organic additions etc. on kinetics of peptide association were monitored~~.

- ~~Fluorescence intensities as measured at 378 nm (monomeric) and 460 nm (associates) were used to characterize the self association of the peptide, $I_E/I_M$ ratio~~.

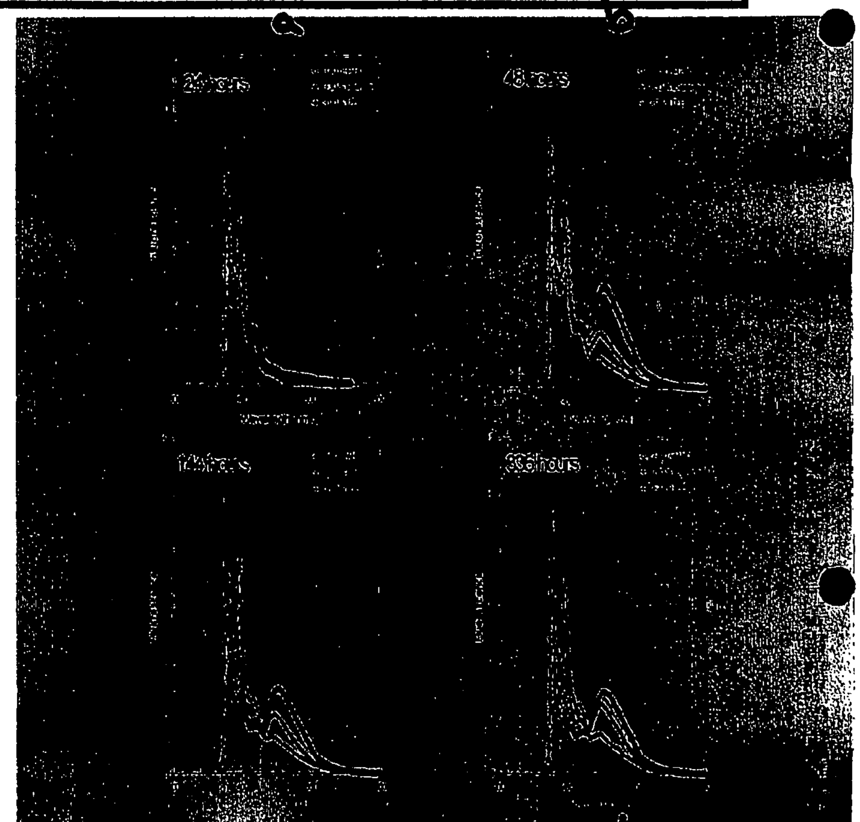




Figure 27

~~Arete Associates~~

# ~~Catalytic Conformational Transition~~ - ~~Effect of Nuclei on Self Association~~

- ~~Insoluble fraction of the peptide was extracted and dissolved in organic solvent (methanol/ethanol/DMF)~~
- ~~Fluorescence of the "insoluble" portion shows high level of peptide association ($I_E/I_M$ ~2)~~
- ~~Small aliquot of the "nuclei" were added to the 20 µM peptide solutions~~
- ~~Presence of nuclei significantly increased the efficiency of peptide association~~

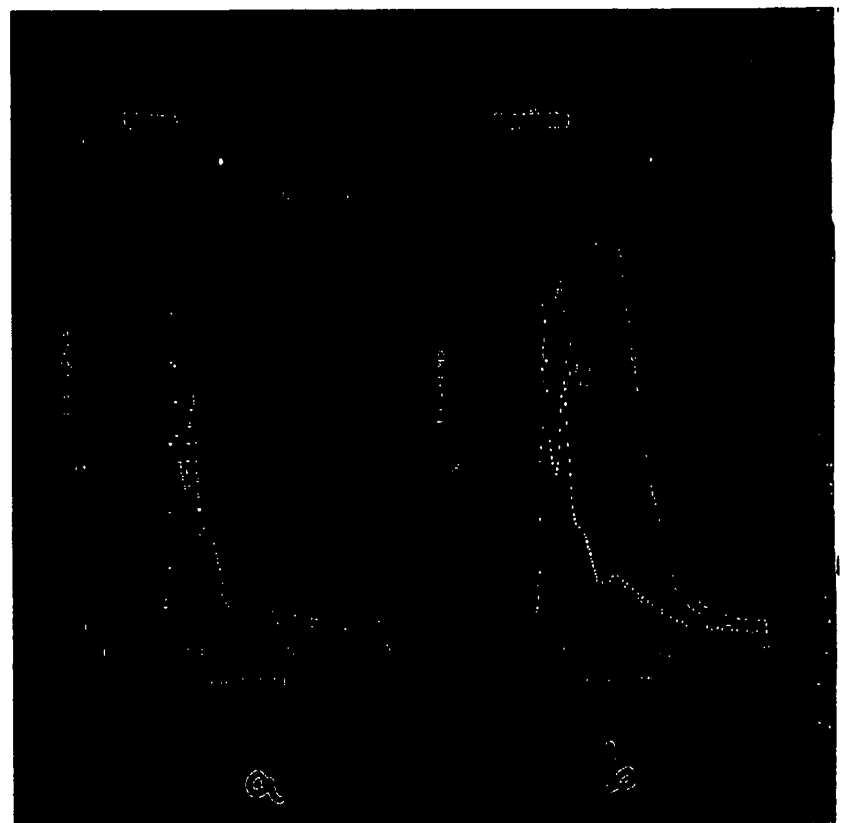



Figure 28

# ~~Generalized Dendrimer Structure~~

KPKTNMKHMAGAAAAGAVV

lys-pro-lys-thr-asn-met-lys-his-met-ala-gly-ala-ala-ala-ala-gly-ala-val-val

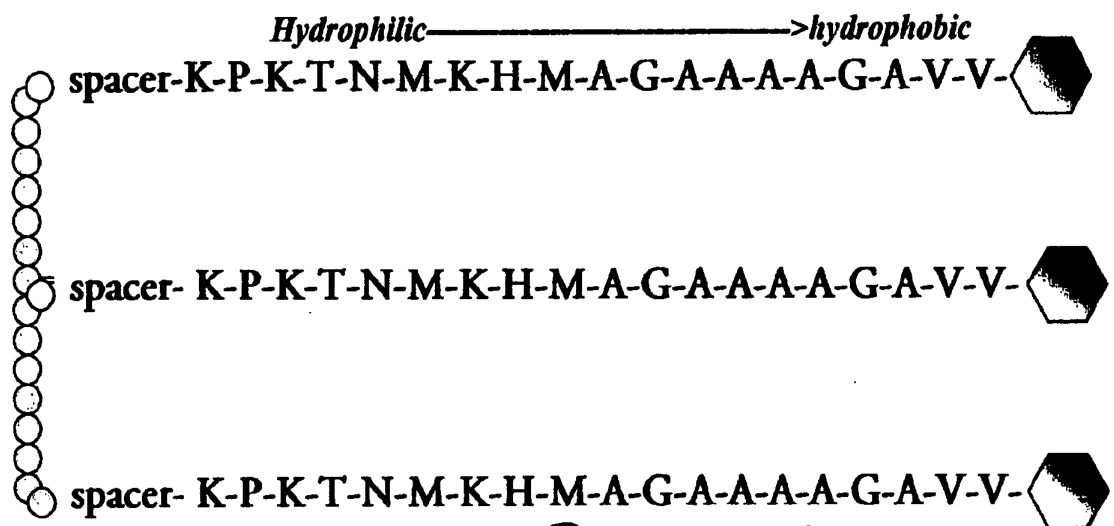


Seq. Id. No. 20

Figure 29

~~Private & Privileged Information~~

# ~~Specific Dendrimer Structure~~

~~Loop-turn-loop or dendrimer to amplify signal and decrease neurotoxicity~~
~~This is the N-terminal segment, probable nucleus for β-sheet transition~~

P~~roposed back-to-back #1 This segment + loop region IS infectious~~ what ~~effect will addition of the mirror segment have? 126-104+109-126~~

~~Change to SS or SSS/AAA?~~ ~~Val-Val--essential to β-sheet formation~~

pyrene VVAGAAAAGAVHKLNTKPK LKHVAGAAAAGAVV pyrene

74

72

~~Loop sequence steric constraints~~
C~~ould add Trp for steric & fluorescence~~

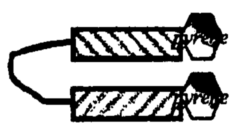

Fig 30a

~~Amyloidogenic palindrome~~

70

~~Green~~ - denotes mouse variants to decrease to~~xicity to humans~~

~~Private & Privileged Information~~

Figure 30

# ~~Experimental Device Concept~~

- ~~Proposed optical device provides for a *simple experimental setup*~~

  — ~~Light source (*blue*)~~
    - ~~lamp~~
    - ~~laser~~

  — ~~T-format sample cell (*gray*)~~

  — ~~Photo-multiplier (*pink*)~~

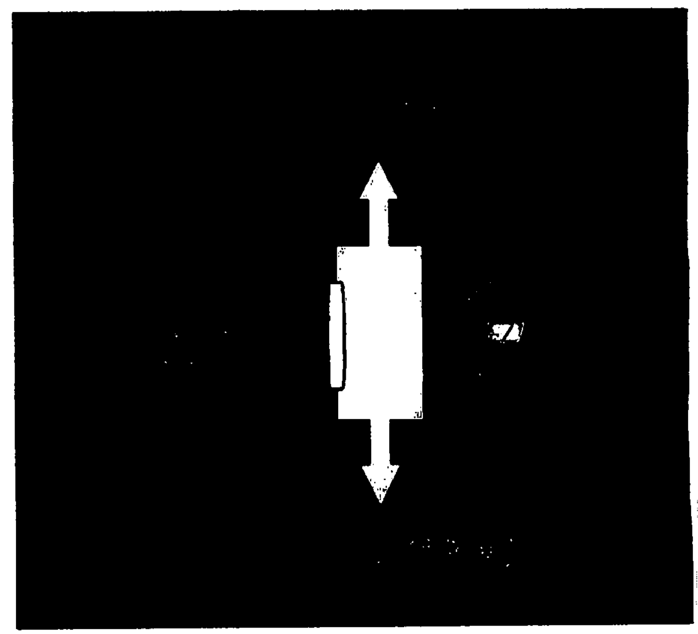

~~Private & Privileged Information~~

Figure 31

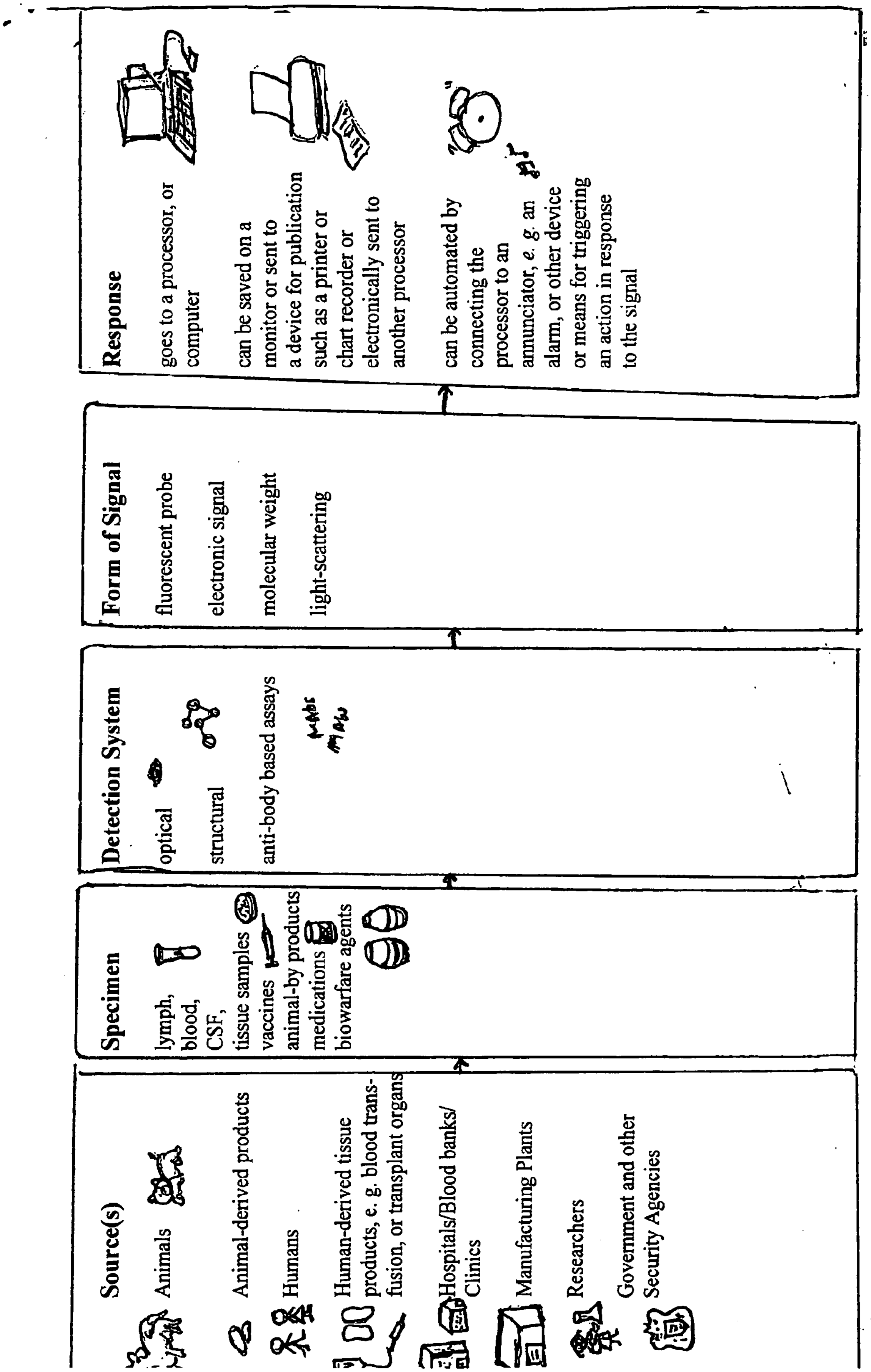
Source(s)
Animals
Animal-derived products
Humans
Human-derived tissue products, e. g. blood trans-fusion, or transplant organs
Hospitals/Blood banks/ Clinics
Manufacturing Plants
Researchers
Government and other Security Agencies
Specimen
lymph, blood, CSF,
tissue samples
vaccines
animal-by products
medications
biowarfare agents
Detection System
optical
structural
anti-body based assays
Form of Signal
fluorescent probe
electronic signal
molecular weight
light-scattering
Response
goes to a processor, or computer
can be saved on a monitor or sent to a device for publication such as a printer or chart recorder or electronically sent to another processor
can be automated by connecting the processor to an annunciator, e. g. an alarm, or other device or means for triggering an action in response to the signal

Figure 32

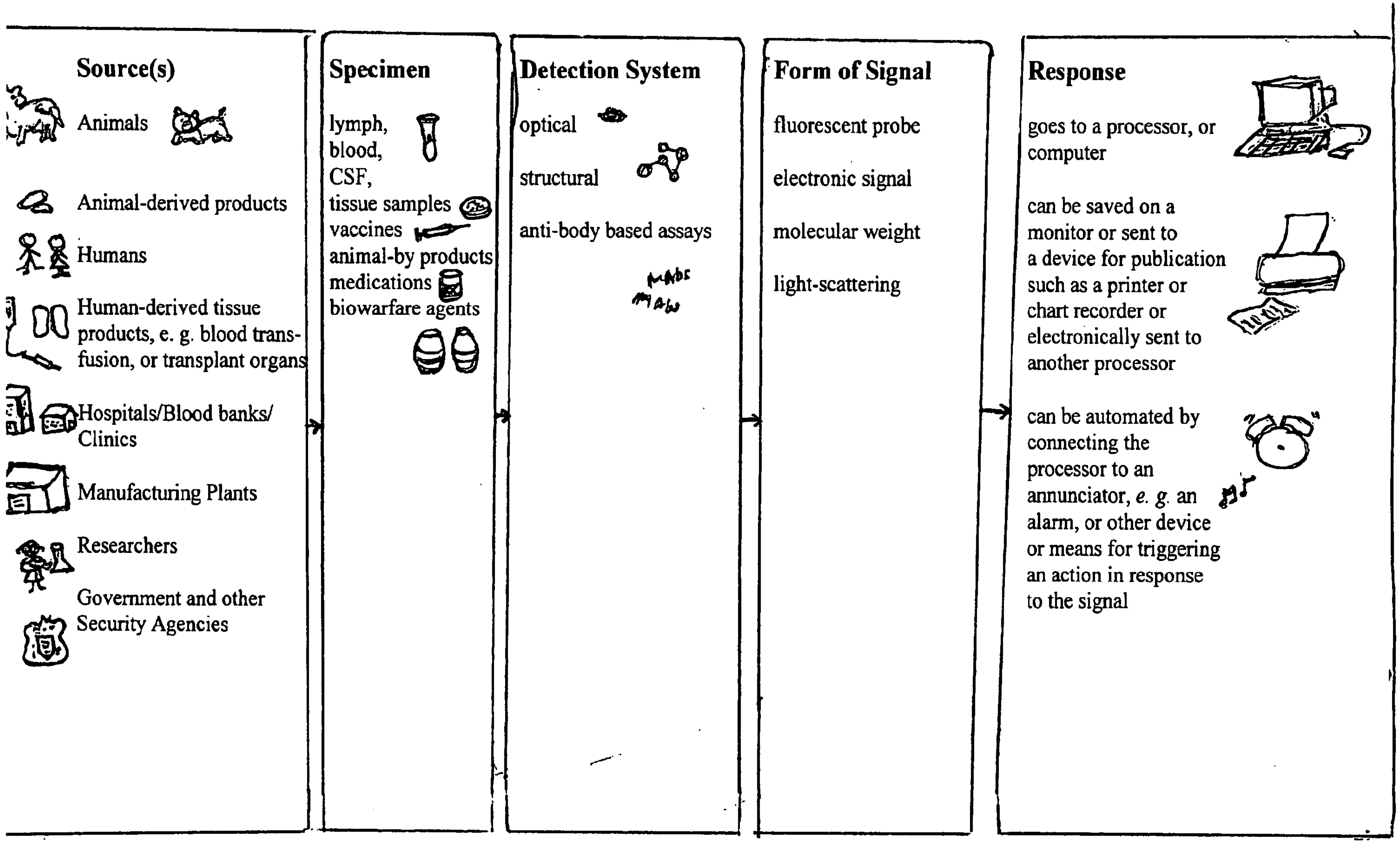
Source(s)
Animals
Animal-derived products
Humans
Human-derived tissue products, e. g. blood trans-fusion, or transplant organs
Hospitals/Blood banks/ Clinics
Manufacturing Plants
Researchers
Government and other Security Agencies
Specimen
lymph, blood, CSF,
tissue samples
vaccines
animal-by products
medications
biowarfare agents
Detection System
optical
structural
anti-body based assays
Form of Signal
fluorescent probe
electronic signal
molecular weight
light-scattering
Response
goes to a processor, or computer
can be saved on a monitor or sent to a device for publication such as a printer or chart recorder or electronically sent to another processor
can be automated by connecting the processor to an annunciator, e. g. an alarm, or other device or means for triggering an action in response to the signal

Figure 32

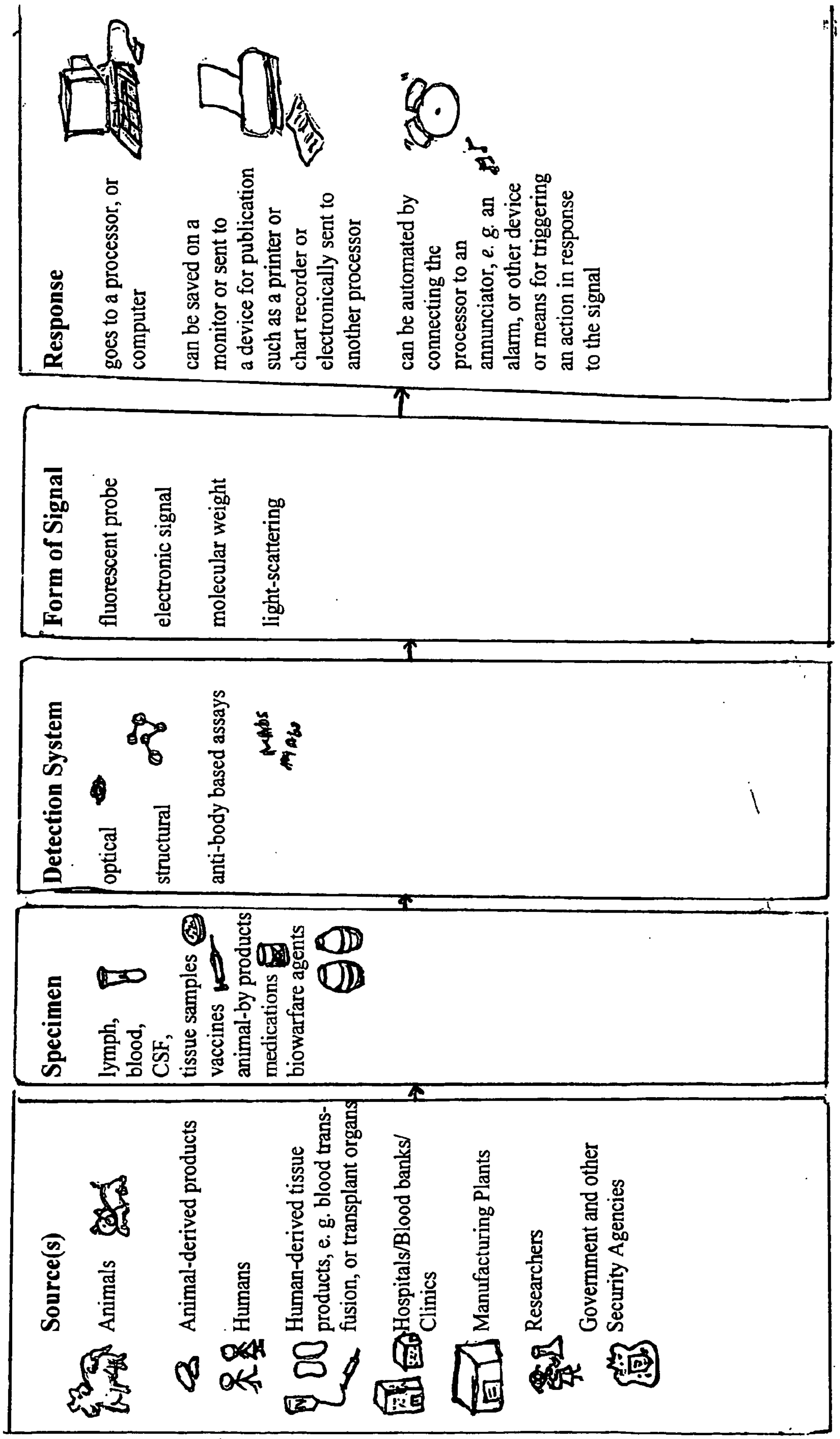
Source(s)
Animals
Animal-derived products
Humans
Human-derived tissue products, e. g. blood trans-fusion, or transplant organs
Hospitals/Blood banks/ Clinics
Manufacturing Plants
Researchers
Government and other Security Agencies
Specimen
lymph, blood, CSF,
tissue samples
vaccines
animal-by products
medications
biowarfare agents
Detection System
optical
structural
anti-body based assays
Form of Signal
fluorescent probe
electronic signal
molecular weight
light-scattering
Response
goes to a processor, or computer
can be saved on a monitor or sent to a device for publication such as a printer or chart recorder or electronically sent to another processor
can be automated by connecting the processor to an annunciator, e. g. an alarm, or other device or means for triggering an action in response to the signal

Figure 32